

IMPLEMENTATION OF THE URBAN CLIMATE MODEL MUKLIMO_3 FOR
BERN AND EVALUATION OF MITIGATION STRATEGIES FOR THE URBAN
HEAT ISLAND

Master thesis

handed in by

Sofya Antonowa

2020

Supervisor:

Prof. Dr. Stefan Brönnimann

-

Advisor:

Moritz Gubler

Content

Abstract	1
1 Introduction	2
2 Urban climate	3
2.1 Urban Heat Islands	4
2.2 UHI mitigation strategies.....	6
2.2.1 White	7
2.2.2 Blue.....	7
2.2.3 Green	8
2.3 Study area	9
3 Data and methods	11
3.1 Muklimo_3	11
3.2 Temperature simulation.....	12
3.3 Input data	14
3.4 Simulation scenarios.....	18
3.5 Evaluation and validation of reference model.....	22
4 Results	23
4.1 Analysis of reference model	25
4.2 Modelled UHI of Bern.....	26
4.3 Evaluation of mitigation strategies	29
4.4 Surrogate climate scenario 2050	29
4.5 Sensitivity analysis	30
4.6 Mitigation strategies of modelling.....	33
4.6.1 Green mitigation strategy	33
4.6.2 White mitigation strategy	36
4.6.3 Blue mitigation strategy	37
4.6.4 Simulation of green chantiers	38
4.6.5 Implementation in urban development	39
5 Discussion	41
6 Conclusion	44
Acknowledgements	46
References	47
Appendix A	55
Appendix B	58
Appendix C	59

Abstract

Bern has already faced extreme temperatures during summer heat waves. The city's UHI and its cause, the heat stress of the city, will only increase due to projected increases in temperature in this area and the strategy of increasing density in built-up thanks to an increasing population by 2050. In addition to that, in its strategies, the city pays special attention to climate research and wants to achieve the reduction of energy consumption. Thus, the evaluation of the UHI and knowledge about most effective mitigation strategies could be applied in sustainable urban planning in the city.

UHI can be studied with field measurements, satellites and models. But only the models can simulate the UHI mitigation strategies.

In this thesis we implement the 3-dimensional urban climate model MUKLIMO_3 for the city of Bern. The simulated UHI effect was evaluated based on the field measurements. The main mitigation strategies, such as green building, the use of high albedo materials and the expansion of water bodies, were modeled and compared.

The simulation was done the 3rd of August 2018, which was the hottest and cloudless day during the 10-days heat wave in summer 2018. The temperature during this day was over 35°C.

The results showed that the model was more accurate during the day compared to night. UHI gains intensity in direction to the city centre and reaches its peak of 2.8°C at night. The white mitigation strategy allows to reduce the temperature by maximum 2°C. The blue strategy reduces the temperature by 2.5°C. The green strategy showed the best results, the temperature can be reduced by 3°C by using it.

The results of this study have good potential for their application in urban planning. They can be used to qualify key guidelines for policy makers, for urban designers, and for architects to reduce the UHI intensity in urban areas and make cities more livable for the residents in the future.

Key words: UHI, mitigation strategy, MUKLIMO_3, city of Bern, temperature

1 Introduction

There is a specific climatological phenomenon in cities wherein the air temperature is higher than in the city's surroundings. This effect called an Urban Heat Island (UHI). Due to urbanization, cities are growing rapidly. Despite the fact that the cities occupy only roughly 3% of the Earth's surface, more than 50% of the population lives in them. The UN (2018) estimates that in 30 years, 68% of the population will be living in cities. That means that there will likely be an increase in urban land area and building density. This could lead to more complex and heterogeneous interactions between urban areas and the atmosphere as well as an increase in UHI intensity. Densely built parts of the inner cities can be more than 10°C warmer than rural areas (US Environmental Protection Agency [EPA], 2008).

The UHI effect is one of the main characteristics of the urban climate (Oke, 1991; Ren & Zhou, 2014). The negative impact of the UHI has been studied for many cities worldwide, and each city has its own characteristics (e.g., with regard to urban forms, topography, regional climate, etc.) (Grize et al., 2005; Cerutti et al., 2006; Aflaki et al., 2017; Geletič et al., 2019). Although it has been known for many decades, it has become a more urgent topic in the context of climate change (Stewart, 2011). The UHIs gets hotter during seasonal heat waves, which leads to health issues (Cerutti et al., 2006; Jiang et al., 2019) and even an increase in deaths in some cases (World Health Organization [WHO], 2009; Ramamurthy & Bou-Zeid, 2016; Jiang et al., 2019) and increased heat stress of the cities (Oke, 1980; Hu et al., 2016; Oke et al., 2017; Li et al., 2020). The heat waves increase in the frequency, duration, and magnitude around the world (WHO, 2009). The UHI intensity is directly related to the size of the city (Oke, 1973), that means that major cities, especially the capitals, are most exposed.

Here, we aim at analyzing UHI in the topographically complex city of Bern, the capital of Switzerland. The city has faced already a heat stress in the summer 2018 (Gehrig et al., 2018; Bader et al., 2018). According to the cantonal scenarios provided by the Federal Statistical Office in Switzerland, the canton of Bern will experience the second largest population growth in Switzerland by 2050, with a projected population of 1,147,000 citizens (Bundesamt für Statistik [BFS], 2020). According to RCP8.5 projection, its temperature will increase by an average of 2-4°C (National Centre for

Climate Services [NCCS], 2018). Besides that, the city is an attractive place for tourism and business development; the center is included in the UNESCO World Heritage List. This leads to the urban development.

The development plans for the city focus on increasing the density of buildings in areas of prospective development called *chantiers* (Stadt Bern, 2017). In its strategies, the city pays special attention to climate research. The city has a new planning guide: their Energy and Climate Strategy 2025 (Stadt Bern, 2015), whose main goals include long-term fulfilment of the 2000 Watt Society standards and for renewable energy sources to account for 70% of the city's heating demand and 80% of its electricity demand by the year 2035. The better understanding the UHI formation in the city and evaluation of effective UHI mitigation strategies could help the city to recline the heat stress and concerning the research (Rosenfeld et al., 1995; Konopacki & Akbari, 2002) to reduce the energy consumption and achieve economic benefits.

The UHI effect can be studied with various methods (Mahdavi et al., 2016). Measurements have the highest precision while satellites have wide coverage. One of the more recent methods is temperature and humidity measurements along paths through the city performed by mobile observations set on bikes (Brandsma & Wolters, 2012; Nemek & Žuvela-Aloise, n.d.). However, simulating the various UHI mitigation strategies and forecasting UHIs for the future is possible only with urban climate models. This method was chosen for this thesis.

The purpose of this thesis is to adapt the parameters of the thermodynamic model MUKLIMO_3 (German Mikroskaliges Urbane KLImaMOdell in 3 dimensions) and to evaluate the modelled spatio-temporal variability of UHI effect in the city of Bern, to compare mitigation strategies (green building, use of materials with high albedos, an increase in bodies of water, etc.). These results may assist in the implementation of improved urban planning in the city to make it more resilient to the heat stress.

This thesis is divided into four sections. The first is an introduction. The second section describes the main problems and the state of urban climate, UHI and mitigation strategies. The third section presents the MUKLIMO_3 model, input data, model initialization, and data evaluation methods. The fourth section presents the results and analysis of the mitigation strategies. The conclusions of this work are then summarized and discussed.

2 Urban climate

The part of the atmosphere where the urban climate is formed is called the urban boundary layer, and the width of it can vary within the span of a day (Oke et al., 2017). Within this layer, there are micro-climatic processes, which are different from the rural due to a considerable disruption of geometry and surface properties of the urban development and changing in the land cover (Oke, 1991). The reduced evaporation due to the lack of vegetation, the low permeability of the underlying surface, and the significant thermal conductivity of the coatings (roofs, building walls, bridges, etc.) of the built-up areas lead to the change in the local temperature, shadow pattern, airflow, and precipitation runoff.

There are five main features that describe the urban climate. First are thermal characteristics such as the UHI effect. The second describes wind, which is related to ventilation and air pollution dispersion. The third is energy, which includes energy balance and partitioning of the urban surface. The fourth is anthropogenic emission, including anthropogenic heat and CO₂ emission. The fifth is water and hydrology features, which are related to precipitation and groundwater balance (Grimmond et al., 2010).

The first two characteristics are most relevant from the perspective of urban design, as they can be largely manipulated by design actions. The first feature, thermal characteristics, is researched in this thesis based on the Muklimo_3 model and described in detail in the next chapter.

2.1 Urban Heat Islands

The UHIs describe the phenomenon of temperatures in the city being noticeably higher than in the surrounding countryside; the difference in temperature can reach more than 10°C (EPA, 2008). The intensity of UHI can be found as the difference between the urban and the rural temperature (Oke, 1987):

$$\text{UHI} := T_{\text{urban}} - T_{\text{rural}} \quad (2.1)$$

The intensity of the UHI changes in time and space under the influence of background meteorological conditions and local features of the city. Most of the city is a 'plateau' of warm air with an increase in temperature toward the city center (figure 2.1). Thermal homogeneity of the plateau is violated by breaks in the general character of the surface in the form of areas of cold such as parks, ponds, and meadows as well as areas of additional heat such as industrial enterprises and dense groups of buildings (Hidalgo et al., 2008). Above the central part of cities is the peak of the heat island, where the air temperature is the highest. In large agglomerations, there may be several such peaks due to the presence of industrial enterprises and dense development (Oke et al., 2017). Large areas of aerodynamic roughness from the underlying surface and the presence of heat islands determine the features of wind conditions of the city.

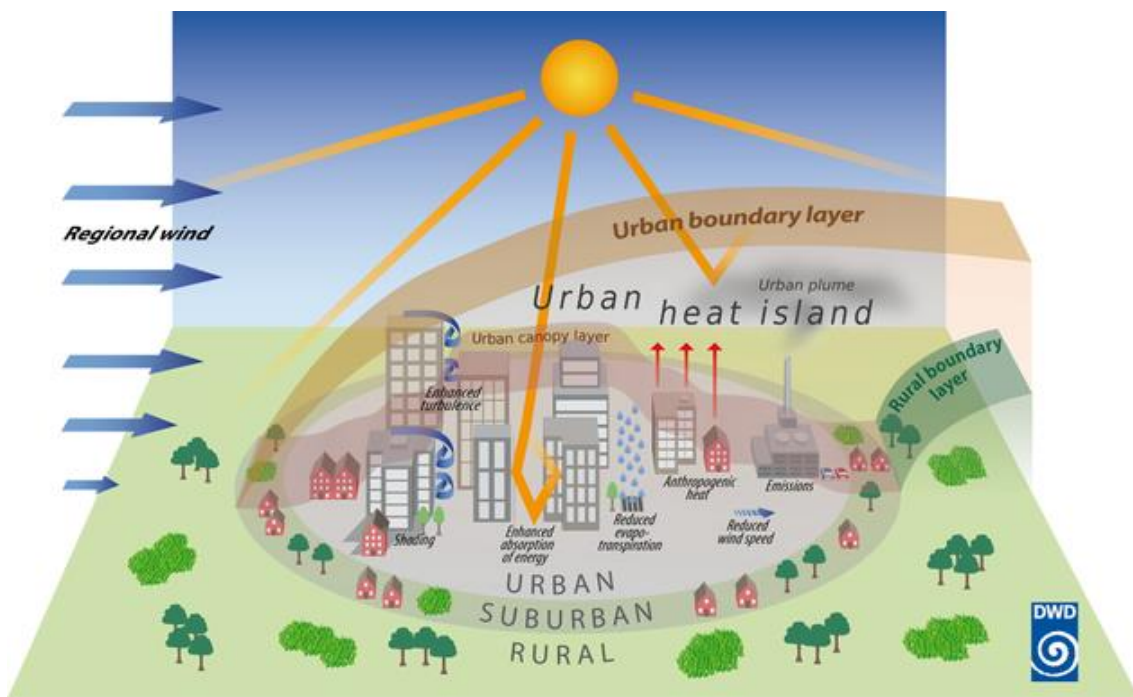


Figure 2.1: Visualization of the UHI phenomenon and influencing factors, "urban heat island" (DWD, 2020)

There several causes of UHI in cities (EPA, 2008). First is the lack of vegetation in the cities; this reduces the cooling effects evaporation and tree shade would have. Second, heat trapped by buildings keeps urban surfaces warmer because built up areas limit the sky view factor and low albedo materials such as dark asphalt and dark roofs trap heat. Next, as a result of anthropogenic activity, there is increased energy consumption for

heating and cooling of buildings and factories. Two primary weather characteristics also affect urban heat island development: wind and cloud cover. In general, urban heat islands form during periods of calm winds and clear skies because these conditions maximize the amount of solar energy reaching urban surfaces and minimize the amount of heat that can be convected away. Climate and topography, which are in part determined by a city's geographic location, influence urban heat island formation. For example, large bodies of water moderate temperatures and can generate winds that convect heat away from cities. Nearby mountains can either block wind from reaching a city or create wind patterns that pass through a city.

There are also several UHI peculiarities that should be taken into account when studying them. First is a UHI's temporal variability: due to lower cooling rates of urban areas compared to rural surroundings, a city's UHI is usually more intense at night (EPA, 2008; Hidalgo et al., 2008; Oke et al., 2017). After sunset, the temperature in rural areas drops to its lowest point. Due to the limited sky view factor, reduced green areas and the accumulated thermal properties of urban materials, the cooling of urban areas slows down. (Oke, 1987). At the same time, the UHI is not uniform and there is a spatial variability. During the day, the difference between urban and rural areas is reduced, but as a result of the difference in albedo in different parts of the city, the diversity of temperatures within the city itself increases (EPA, 2008). In addition to temporal and spatial variation, there is also variability between seasons. In mid-latitudes, UHIs are most intense in summer due to increased solar radiation. (Oke, 1982).

2.2 UHI mitigation strategies

The UHI effect can be minimized with several mitigation strategies such as using the high-albedo materials, planting more vegetation or setting additional water bodies (Musco, 2016; Perez, 2018; Alexandrovich et al., 2017). They are called the white, green, and blue mitigation strategies, respectively. By applying the urban climate model Muklimo_3 and setting different conditions in the model, we can see how these strategies would affect UHI intensity in the city.

2.2.1 White

The white mitigation strategy is described by applying the high albedo materials by developing the city. Sailor (1995) and Taha (1997) found that materials with high albedo can reduce UHI. The use of high albedo materials of pavement, roofs, walls etc. increase the reflection of the light energy, so the absorbed solar energy doesn't convert into the heat and the surface doesn't warm up. Albedo can be measured from 0 to 1. Zero characterizes black (known as black body radiation) and has 0% reflection, so all solar radiation is absorbed while one characterizes white, which has 100% reflection.

High albedo materials are usually implemented in roofs, walls, or pavements (O'Malley et al., 2015). Simple white paint sprayed on to a test section can reduce the temperature by 10 to 15 °C (Breslin, 2018).

White strategies are justified when creating new districts and quarters, but when renovating old buildings, it would be necessary to adjust projects. There are some drawbacks of a white strategy, including the high cost of new materials and the fact that the use of highly reflective materials can lead to eye problems for citizens (when they reflect too brightly). Additionally, when the reflected rays are superimposed on each other, local heating of nearby surfaces can occur, causing damage (Aleksandrowicz et al., 2017).

2.2.2 Blue

The blue strategy is characterized by introducing new bodies of water into an urban area. It was concluded that bodies of water help to minimize UHI effects in the city (Coutts et al., 2012). The evaporative cooling effect from bodies of water is achieved by the transformation of the sensible heating produced from absorbed thermal energy to latent heating with the production of water vapor (Oke, 1987). However, closed bodies of water such as lakes are the buffer of the daily temperature cycle: they cool the environment during the day and heat it up at night, which adversely affects thermal comfort (Theeuwes, 2013).

There are many successful examples of applying the blue strategy in the cities, such as the Walthamstow Wetlands in London, UK or a cascade fountain, Kharkov, Ukraine. The

additional water bodies in a city can provide a cooling effect of 2.5°C on average (Volker et al., 2013). Besides the cooling effect, the blue strategy has recreational benefits, but it requires space, which big cities tend to lack.

2.2.3 Green

The green strategy includes green technologies and vegetation. During the photosynthesis process, vegetation converts water, carbon dioxide, and solar radiation to glucose and oxygen (Rosenfeld et al., 1995). Due to evaporation, the absorbed energy of solar radiation converts into heat, leading to air temperature mitigation and relative humidity enrichment. The plants shade the urban surfaces and protect them from the solar radiation thus from heating. They also increase surface roughness and thus improve convection. Additionally, the green strategy helps to mitigate air pollution, improve management of run-off water, improve public health, and enhance the aesthetic value of the urban environment (Arabi et al., 2015).

The green strategy is usually applied to roofs and walls as well as through the addition of more green spaces. Niachou et al. (2001) examined green roofing and its thermal properties. They found that such green roofs cool down the temperature in summer. This cooling effect was noticeable during daytime and was even higher at night. This is due to both the effect of cooling green roofs at night, and the natural cooling of the air in the lack of light radiation. Robitu et al. (2006) found that vegetation can save up to 10% buildings' cooling costs. Wong et al. (2011) also confirmed the benefits from vertical greenery as control temperature and limit energy consumption. Shashua-Bar & Hoffman (2000) found that parks and green areas have a positive effect in reducing temperatures as they cause evapotranspiration along with shading. This effect leads towards the cooling island effect in the city and it can reduce UHI intensity by 3°C (Rodatz, 2012).

However, there are also a number of disadvantages of this strategy: trees must be adapted to the climatic conditions of the area, and it takes a long time for the trees to grow.

2.3 Study area

The city of Bern is the capital of Switzerland. It is the fifth most populous city in Switzerland. About 143,000 people are living here, according to the federal statistical office, and 160,000 people are projected to be living in the city and more than 1 million in the canton by 2050 (Bundesamt für Statistik [BFS], 2020). Historically, the city was built on a high hill in the bend of the Aare River, which now crosses the city and splits it into a western and an eastern part. The center of the city is listed as a UNESCO World Heritage Site.

Geographically, the city of Bern is located in a basin in the transition area between higher and lower central swiss plateau. The topography of the city is heterogenous (figure 2.2). The city is surrounded by several hills. Among them are the Könizberg (674 m.a.s.l.) on the south-west, the Gurten (858 m.a.s.l.) on the south, the Dentenberg (740 m.a.s.l.) on the south-west and the Bantiger (947 m.a.s.l.) on the north-east. The location creates frequent calm and inversions in the city, which leads to temperature drops in the lower parts of the city (Mathys,1980). There are two main wind directions north-east and south-west ,but the location of the river basin creates a very difficult wind situation, especially near the center of the city.



Figure 2.2: Location of the city of Bern (© Data: swisstopo)

The city positions itself as an interesting place for tourism and business. Development plans for the city focus on increasing the density of buildings in areas of prospective development called *chantiers* (Stadt Bern, 2017). Building density can increase the impact of thermal stress.

The partial revision of building norms and rules of use, the cessation of urban expansion, and the development of internal settlements serves as the target of urban planning in Bern (Stadt Bern, 2017). The quality of life and adaptation to the climate are planned in detail (Stadt Bern, 2020). This will lead to compaction of city development and probably to an increase in the UHI's area.

One of the most important urban planning strategies in Bern is *chantier* planning. *Chantiers* are stable development areas with high spatial quality. They are strategically important areas in Bern that have special potential for modernization and development (Stadt Bern, 2017). The city is planning twelve *chantiers* (Figure 2.3) which are located in all five districts of the city except the city center.

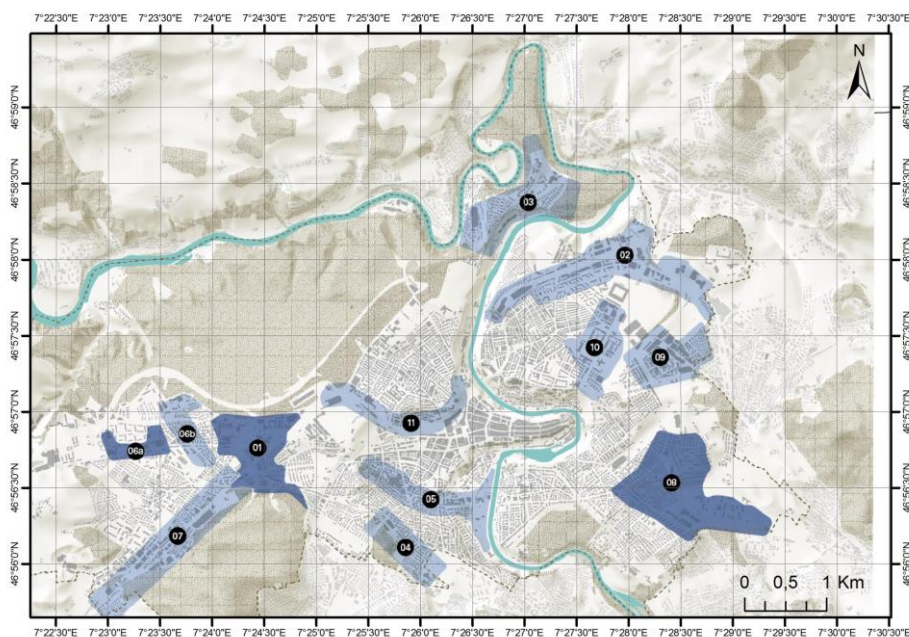


Figure 2.3: The twelve chantiers, which are planned to develop by 2025. 01 Ausserholligen; 02 Wankdorf; 03 Tiefenau-Relsenau; 04 Weissenbühl; 05 Corridor Eigerstrasse; 06a Bethlehem West; 06b Bethlehem East; 07 Corridor Freiburgstrasse; 08 Corridor A6 South; 09 Galgenfeld; 10 Kasernenareal; 11 Belvédère Länggasse (Stadt Bern, n.d.)

All of the facts mentioned above play both a direct and indirect role in UHI formation in the city. Being a UNESCO World Heritage Site means that the application of some mitigation strategies is limited (eg. changing the albedo or increasing the area of bodies of water, resulting in architectural changes in the city center).

3 Data and methods

3.1 Muklimo_3

In this thesis, we used a 3D non-hydrostatic micro-scale urban climate model, MUKLIMO_3, which was developed by Deutscher Wetterdienst (DWD) for micro-scale urban climate and planning applications (Sivers & Zdunkowski, 1986). The thermodynamic version of the MUKLIMO_3 is able to provide a tool for various scientific applications on an urban scale such as urban flow, cold air removal, and urban heat islands. The MUKLIMO_3 simulates atmospheric temperature, humidity, and wind field on a three-dimensional model grid. For this purpose, the model has been supplemented with prognostic equations for atmospheric temperature and humidity, a momentum balance of heat and moisture in soil, and a complex model of vegetation (Sievers, 1995). Cloud processes and precipitation are not considered, which limits the application of the model to days without precipitation.

Urban climate model Muklimo_3 works in two phases. In the first phase, the day before the start of the 3D model, the 1D model is launched. It indicates the boundaries and a stable vertical profile of temperature and humidity, as well as the profile of ground variables for each corner of the modeled area. The wind direction and speed at this stage is a constant.

In the second phase, having obtained the initial data of the stationary profiles, Muklimo_3 runs a 3D model in parallel with its 1D work. The 1D model results are used to continuously update the values of the 3D model running at the edges. At this stage, the 1D model also provides incoming shortwave and longwave radiation on the ground of the model section. The 1D model provides additional information about the type of soil cover, initial soil water content, and average soil compaction.

The equations of heat and humidity balance in the atmosphere allow Muklimo_3 to calculate a given period of time. At this stage, the model also connects data from a land use classes presented in the land use table. The 3D modelling result is a four-dimensional field for atmospheric variables and soil layers. For the period under review,

which usually covers 24 hours, changes in the variables are simulated hourly for each grid cell.

MUKLIMO_3 is able to account for plants and buildings via different parameterizations in order to simulate various scenarios of temperature, wind and moisture. The main differences between "non-building" grid points and unresolved building grid points are reduced atmospheric pressure, moisture and temperature exchange between the building and the atmosphere, modified turbulent exchange, and wind field disturbance.

MUKLIMO_3 can also parametrize the radiation, which is done separately for longwave and shortwave radiation. Longwave radiation is considered to be coming from the buildings and soil while shortwave radiation is parametrized by the following inputs: sun angle, sun zenith, solar constant, and atmospheric turbidity (Verein Deutsche Ingenieure, 1994). This type of radiation is modelled to be absorbed and reflected by the buildings, soil, and trees. The albedo for the buildings is set in the land use table.

Building shade also has an impact on the shortwave radiation balance. Therefore, its impact on the soil is reduced in the grid points with buildings. Leaf area density and leaf area indices are used to model the shortwave radiation impact (both absorption and reflection) on trees and the canopy layer respectively. MUKLIMO_3 has a canopy parametrization model. This is needed to model the heat and moisture exchange between the plants and the atmosphere because the leaves block a part of the airflow and reduce the radiation and moisture. There are three layers of plants set: tree top, tree stem, and canopy (heights are set in the land use table).

3.2 Temperature simulation

MUKLIMO_3 is used for thermal field forecasts, which allows modelling the city and its surroundings on an urban scale (Sievers, 1995). The basic version of MUKLIMO_3 solves the Navier-Stokes equations for modelling fields of atmospheric flows. It is based on the two-dimensional atmospheric model of MUKLIMO (Sievers & Zdunkovsky, 1986) with a generalization of the flux-vortex function method to three dimensions.

The thermodynamic version can simulate diurnal variations of temperature and relative humidity, which simulate the potential temperature and consider different canopy-layer and building conditions. In this manner, the model becomes an atmospheric model with restrictions to the boundary conditions given by the 1D model.

The output data of the model are temperature fields. To estimate the impact of urban warming, the data should be compared with the temperature outside the city. The UHI is the temperature difference between the model and the Zollikofen weather station. The procedure of UHI intensity calculation from 1D modelling is shown in figure 3.1.

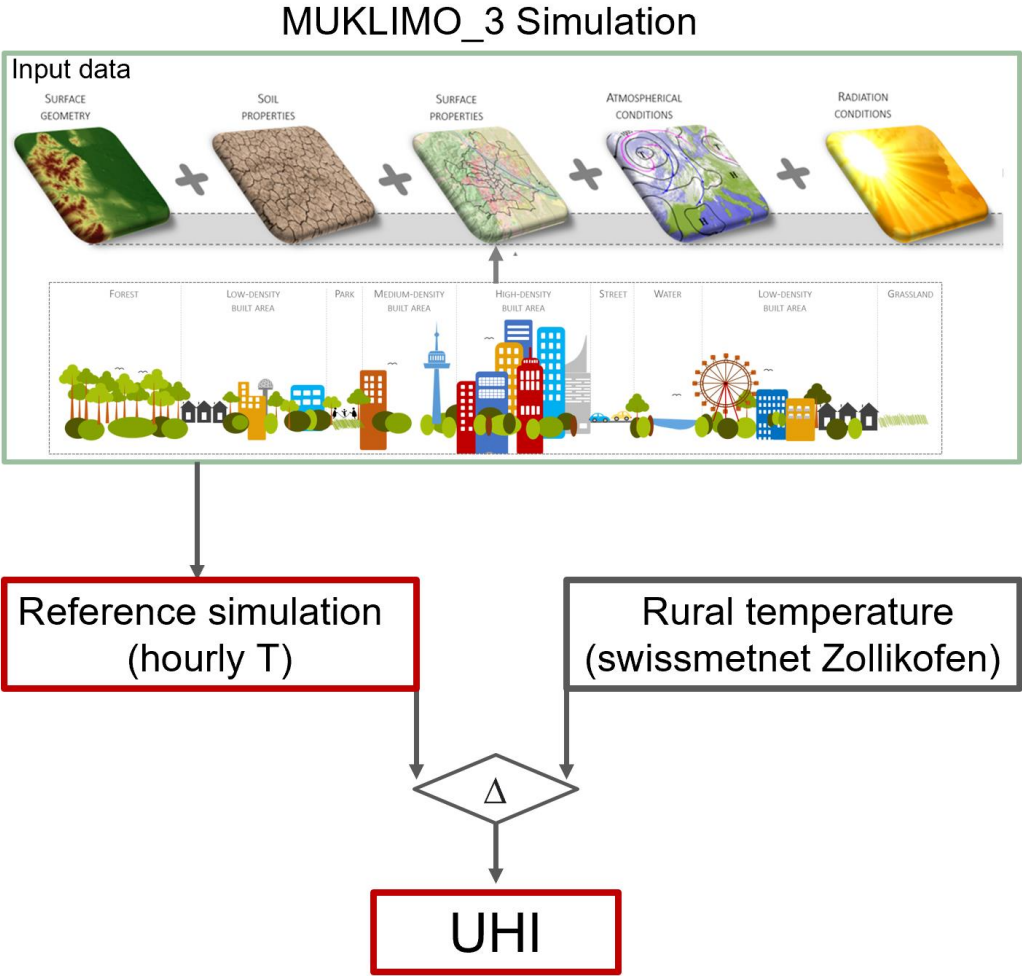


Figure 3.1: The UHI intensity calculation procedure from 1D modelling. The UHI is calculated as the difference between a 24-hour modelling cycle of MUKLIMO_3 simulated fields to the ambient temperature and weather data stations

3.3 Input data for MUKLIMO_3

Data concerning the surface geometry, surface properties, atmospheric conditions, soil properties, and radiation conditions of the study area are required to parametrize and run the model.

The data of surface geometry consist of the size and location of the study area. For this study, a field of 11200m*6200m was selected (224*124 grid cells, size of grid cells being 50m*50m), capturing Bern and its three major municipalities: Muri bei Bern, Köniz, and Ostermundigen. The parameter related to the modelling height was set 3 m above the ground surface. This corresponds to the height of the data taken by the field measurements.

The swisstopo raster data of the digital elevation model (with 25 m resolution) was provided by the Institute of Geography at the University of Bern. The raster data are formatted in ArcGIS and then converted to ASCII format. The height difference in the study area varies from 478 m above sea level to 826 m above sea level.

Atmospheric conditions were described by meteorological parameters. The meteorological data such as surface temperature, wind speed and direction, and humidity were taken in this study from the Zollikofen weather station (7°27'53E 46°59'31N WGS84). The station is located in a rural area about 5 km north of the city center (figure 3.2). The data for the vertical temperature profile were taken from the radio-sounding observation for the Payerne station provided by the Department of Atmospheric Science at the University of Wyoming (University of Wyoming, n.d.)

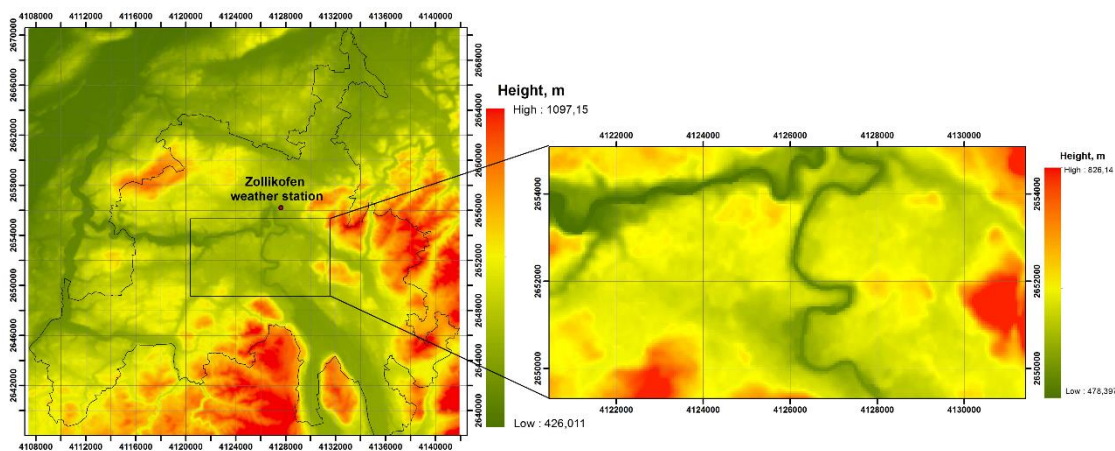


Figure 3.2: Selected study area with topography and the Zollikofen reference meteorological station

August 3rd, 2018 was chosen for simulation for a couple of reasons: it was the hottest day during a 10-daily heat wave, and it was entirely sunny without any precipitation or clouds (figure 3.3), which is important because the Muklimo_3 model does not allow phase transitions of water. Precipitation and cloud formation are therefore not possible (Sievers, 2017).

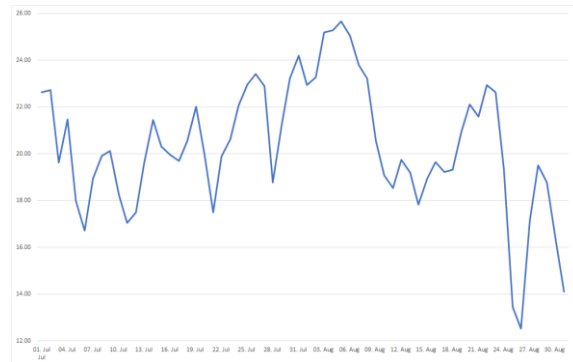


Figure 3.3: The mean daily temperature from July 1st, 2018 to August 30th, 2018 with the highest mean daily temperature on August 3rd, 2018.

The model provides various settings for 12 classes for soil textures as defined by the United States Department of Agriculture (Sievers, 2017) such as soil moisture, volumetric porosity, and soil sealing. Sandy loam soil was chosen as the most suitable for the study area.

To run the MUKLIMO_3 simulation, the model needs land use data of the city. Information about buildings such as height and fraction as well as information about trees and the canopy layer must be detected and converted into information that the model can process. For a more accurate calculation, the land cover data for the Canton of Bern were simulated in the standard European land cover data called Urban Atlas provided by the Copernicus Land Monitoring Service (Copernicus, 2020). These data include 27 land use classes, which are represented as seamless vector data with horizontal resolution from 100 to 250 m (Figure 3.4 and 3.5).

By starting the simulation, the model combines these data with a land use table (Tab. 3.1 and 3.2) for each of the 27 land use classes. The parameters are divided into two groups related to buildings or to vegetation. The first group requires parameters of building area, building height, wall area index, and roughness. Tree height, leaf surface density, leaf area index, soil cover are required for the second group. Albedo parameters belonging to both groups are also available. In one land use class, there can be either

buildings or trees, which means that trees between buildings or inner yards with tree are not taken into account by the model, so that may lead to much uncertainty.

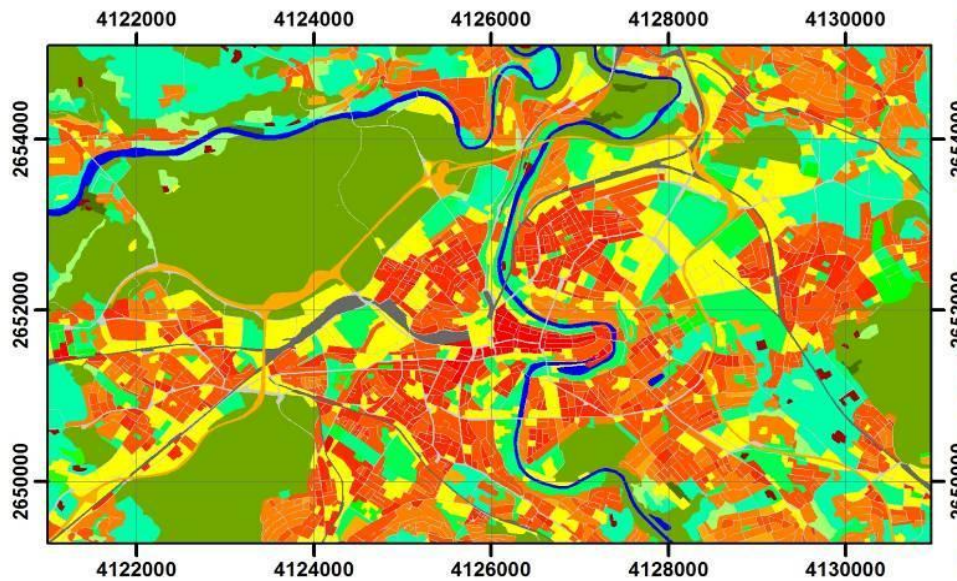


Figure 3.4: The colors represent the land use classes

- 01:Continuous urban fabric (S.L. : > 80%)
- 02:Discontinuous dense urban fabric (S.L. : 50% - 80%)
- 03:Discontinuous medium density urban fabric (S.L. : 30% - 50%)
- 04:Discontinuous low-density urban fabric (S.L. : 10% - 30%)
- 05:Discontinuous very low-density urban fabric (S.L. : < 10%)
- 06:Isolated structures
- 07:Industrial, commercial, public, military, and private units
- 08:Fast transit roads and associated land
- 09:Other roads and associated land
- 10:Railways and associated land
- 12:Airports
- 13:Mineral extraction and dump sites
- 14:Construction sites
- 15:Land without current use
- 16:Green urban areas
- 17:Sports and leisure facilities
- 18:Arable land (annual crops)
- 19:Permanent crops (vineyards, fruit trees, olive groves)
- 20:Pastures
- 21:Complex and mixed cultivation patterns
- 23:Forests
- 24:Herbaceous vegetation associations (natural grassland, moors...)
- 25:Open spaces with little or no vegetation (beaches, dunes, bare rocks, glaciers)
- 26:Wetlands
- 27:Water

Figure 3.5: Color, number, and a short description of each land use class

Table 3.1: *The simulated parameters*

Parameter	Description
vg	Fraction of type buildings on study area
wai	Wall area index, which determines the ratio of the wall area of a building to its study area
h	Height of the buildings
vs	Degree of sealing (0 - 1) of all areas between the buildings, special allocation: vs = -1 for water bodies
z0	Roughness length in m of building free areas and areas under trees, respectively
hbm	Height of trees in m
hast	Height of the tree trunk in m
bf0	Leaf area density in of the tree trunk in m ⁻¹ of one tree
bf1	Leaf area density of the tree top in m ⁻¹ , based on one single tree
lai	Leaf area index of a single plant in the canopy layer
hca	Height of natural vegetation in the canopy layer in m
sigbm	Fraction of trees
sigma	Fraction of natural vegetation in the canopy layer

Table 3.2: *Parameters of the land use classes*

№	vg1	wai1	h1	vs	z0	hbm	hst	bf0	bf1	lai	hca	sigbm	sigma
1	0.28	2.1	18	0.79	0.2	0	0	0	0	0.9	0.4	0	0.33
2	0.37	3.2	13	0.29	0.2	0	0	0	0	1	0.4	0	0.22
3	0.2	1.8	7	0.18	0.2	0	0	0	0	1	0.5	0	0.23
4	0.14	1.7	5	0.01	0.2	0	0	0	0	0.8	0.4	0	0.23
5	0.06	1.2	4	0.02	0.2	0	0	0	0	1.1	0.5	0	0.33
6	0.07	1.3	9	0	0.2	0	0	0	0	0.9	0.5	0	0.3
7	0.31	0.9	7	0.54	0.2	0	0	0	0	1	0.4	0	0.34
8	0	0	0	0.51	0.1	7	3	0.05	0.8	0.8	0.3	0.11	0.23
9	0	0	0	0.42	0.1	9	4	0.05	0.8	0.8	0.4	0.1	0.38
10	0	0	0	0.5	0.1	9	4	0.05	0.8	0.9	0.4	0.03	0.41
11	0	1.3	5	0	0.1	0	0	0	0	0.9	0.3	0	0.11
12	0.2	1.9	4	0.24	0.2	0	0	0	0	0.7	0.2	0	0.57
13	10.05	0.5	6	0.3	0.2	0	0	0	0	1	0.4	0	0.17
14	0.09	0.9	6	0.29	0.2	0	0	0	0	1	0.4	0	0.08
15	0	0	2	0.25	0.2	5	2	0.05	0.8	0.9	0.5	0.08	0.72
16	0	0	0	0.14	0.2	10	5	0.05	0.8	0.9	0.4	0.34	0.87
17	0	0	0	0.23	0.2	10	5	0.05	0.8	0.9	0.3	0.07	0.7
18	0	0	0	0.04	0.1	7	3	0.05	0.8	1	0.5	0.13	0.9
19	0	0	0	0	0.2	7	3	0.05	0.8	0.9	1	0.05	0.9
20	0	0	0	0.05	0.1	7	3	0.05	0.8	0.8	0.5	0.03	0.9
21	0	0	0	0.05	0.1	7	3	0.05	0.8	0.8	0.5	0.03	0.9
22	0	0	0	0.04	0.1	7	3	0.05	0.8	0.8	0.5	0.03	0.9
23	0	0	0	0	0.2	20	8	0.05	0.8	1.5	1	0.59	0.73
24	0	0	0	0	0.2	11	5	0.05	0.8	0.7	0.5	0.16	1.07
25	0	0	0	0	0.1	0	0	0	0	0.8	0.4	0	0
26	0	0	0	-1	0	0	0	0	0	0.8	0.6	0	0
27	0	0	0	-1	0	0	0	0	0	0.9	0.5	0	0

3.4 Simulation scenarios

The simulation which was performed on August 3rd, 2018 has received 25 rasters of absolute temperature distribution with one-hour time intervals (time levels in MESZ hh.mm (1... 25) 09:00, 10:00, 11:00, 12:00, 13:00, 14:00, 15:00, 16:00, 17:00, 18:00, 19:00, 20:00, 21:00, 22:00, 23:00, 00:00, 01:00, 02:00, 03:00, 04:00, 05:00, 06:00, 07:00, 08:00, 09:00; see figures in appendix A). Visually, the difference is almost invisible. Therefore, temperature simulations with intervals of only an hour are insignificant. For the greatest contrast, one should take only 4-time intervals. At 12:00, the solar radiation reaches its peak. At 16:00, the ground warms up the most. At 03:00, solar radiation is zero. At 07:00, the lowest surface temperature is recorded. Thus, four points in time were chose for time sensitivity analysis (12:00, 16:00, 03:00, and 07:00). In the remainder of the text, 12:00 and 16:00 refer to the daytime heating effect (day), and 03:00 and 07:00 refers to the effect of nocturnal cooling (night).The initial model calculated time points 12:00, 16:00, 03:00, and 07:00 for August 3rd, 2018.

The basis of modelling was August 3rd, 2018. This was the fifth day of the 10-day heat wave in summer 2018. This model is called the reference model (REF). Its parameters were corrected so that the difference between the field measurements and the model data was minimal. All input data previously described was used, the initial temperature was 22°C., the soil 22°C and the water 18°C. the wind direction was SW with a wind speed of 2.6 m/s.

Two-day period simulations (S2D) were performed to test time sensitivity from August 3rd, 2018 to August 4th, 2018. The task was to analyze the effects of the duration of day modulation on the result.

The REF simulation was done with two wind directions and speeds (Wdf). The south-west wind had a speed of 2.6 m/s (SW). The north-east wind had a speed of 0.5 m/s (NE). Wind is one of parameter that impacts temperature creation. The task was to analyze the influence of wind direction and strength on the result.

The spatial distribution of the temperature increase was simulated in accordance with the data of RCP8.5 scenario of the projection CH2018 (National Centre for Climate Services [NCCS], 2018. The surrogate climate change scenario 2050 (S2050) was

performed with the input data of the reference day with increased initial temperature on 4°C.

The three mitigation strategies (white, blue, and green) were simulated relative to the reference day (August 3rd, 2018) with different land-cover strategies.

In the white strategy (ALB), the albedo parameter was increased to 0.5-0.7 units for the first 7 classes in the land use table 3.3.

In the blue strategy (BL), small water areas were added to the land use class approximately equidistant throughout the study area. These included impenetrable water bodies (lakes), cascading waterfalls, swimming pools on roofs, and other irrigation systems. The water area increased by 3.8% relative to the whole study area.

In the green strategy (GR), small green areas were added to the land use class approximately evenly throughout the study area. The increase of forested area was 6% relative to the whole study area. Spatial changes are shown in the figure 5.3.

In order to evaluate the maximum temperature deviations from the reference, two extreme models were simulated. The first was a model completely without forest (NOGR). The land use class "forest" was replaced by the seventh land use class which is called "industrial, commercial, public, military and private units", and it subtracted 21% of green areas from the whole study area. The second simulation was with an Ideal Forest (IGR), where the first 7 land use classes of urban fabric types were replaced by "forest" land use, meaning the use of green technologies in construction. The forest area increased by 54% from the set research area.

Chantiers are areas of perspective development of the city. In order to assess the real impact of the "green strategy" model, a simulation was done in which the *chantier* areas were replaced by "urban green spaces" (SCH). This implies that the *chantier* would be built using only green technologies and energy efficient materials. The main features of the reference and mitigating models are presented in tables 3.3 and 3.4

Table 3.3: Features of reference and mitigating strategies

abbreviation	description	changed in relation to REF
REF	reference simulation 03.08.2018	see Appendix
S2050	modelling of surrogate climate change scenario 2050	increased initial air, water and soil temperature by 4 C
S2D	two-day simulation	increased time period
WDF	simulation of 2 wind directions	wind speed NE; wind speed 0.5 m/s
GR	green mitigation strategy	increased of the area of "forest" land use class by 6% (to 27% in relation to whole study area accordingly)
ALB	white mitigation strategy	increased albedo to 0.7 by "buildings" and "airport" land use classes; to 0.5 by roads land use classes
BL	blue mitigation strategy	increased of the area of "water" land use class by 3.8% (to 5.6% in relation to whole study area accordingly)
NOGR	simulation without forest	land use "forest" was replaced by 7th land use class which is called "Industrial. commercial. public. military and private units" minus 21% of green spaces from the whole study area
IGR	simulation with forest	increased of the area of "forest" land use class by 35% (to 54% in relation to whole study area accordingly) 1-7 land use classes were replaced by land use "forest"
SCH	simulation of green <i>chantiers</i>	all classes included in <i>chantiers</i> have been replaced by "urban green space" land use class

Table 3.4: Initial and final states of the simulated parameters

Study area	The studied area 50m*224 cells*50m*124 cells=69 440 000 m ²
Water	Area under water was 50*50*507 cells=1267500 m ²
	Water area became 50*50*1570 cells=3925000 m ²
	This is 1.8% and 5.6% of the study area, accordingly.
Forests	The area under the forests was 50*50*6044=15110000 m ² .
	The area under the forests became 50*50*7532=18830000 m ² .
<i>Chantier</i>	<i>Chantier</i> area 8337060 m ²
	Green urban areas were 10470000-8337060=2132940 m ²
	Green urban areas became 50*50*4188=10470000 m ² .
	This is 3% and 15% of the study area. (increase in green urban areas by 12%)

Initial spatial data for different strategies is shown in the figure 3.6.

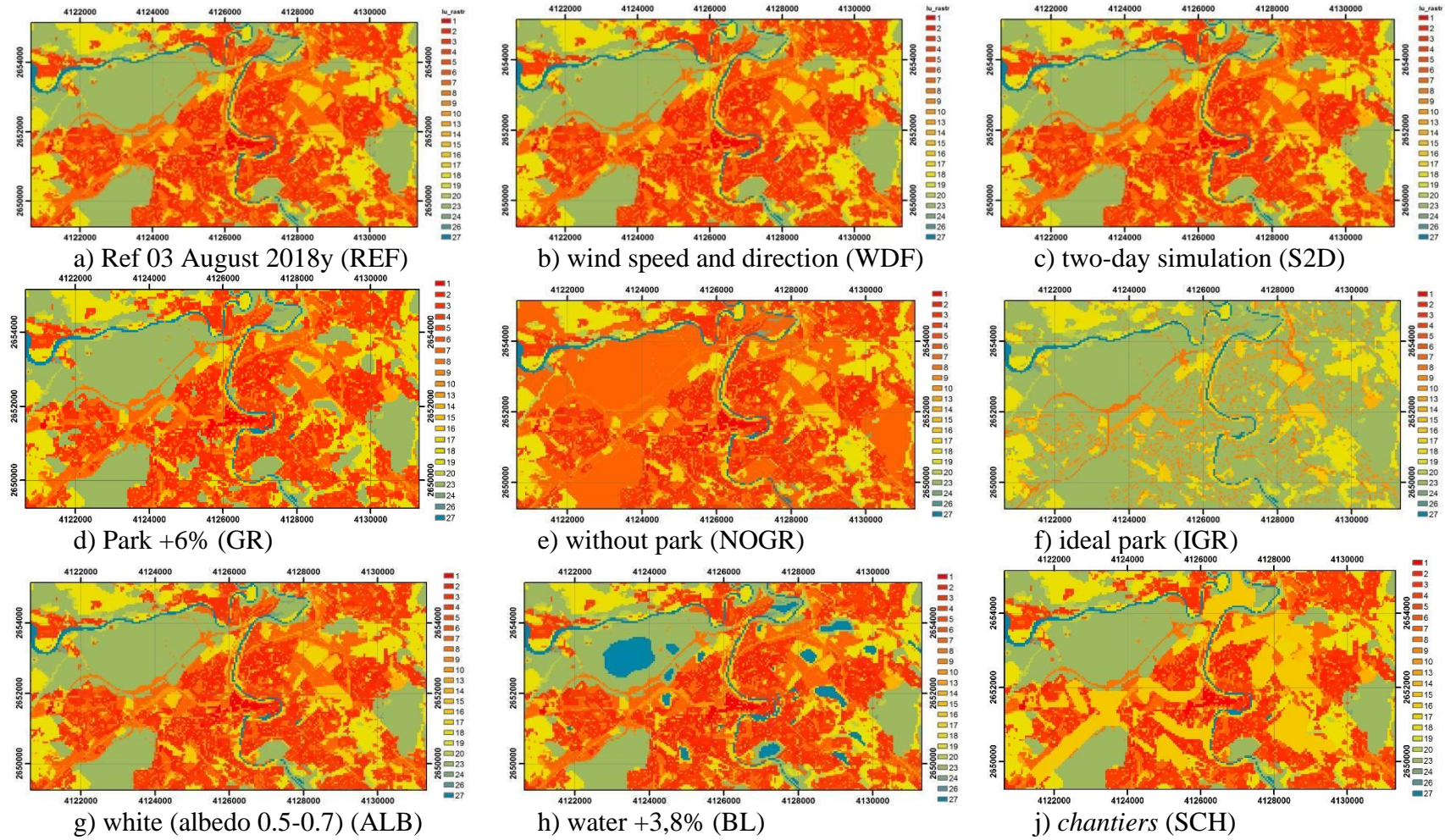


Figure 3.6: Land use data. a) Normal Land use (REF); b) wind speed and direction c) two-day simulation; d) Land use with an increase the parks area by 6% (GR); e) without park (NOGR); f) green building (IGR); g) white strategy (ALB); h) blue strategy BL (increase water body by 6%); i) chantiers (SCH)

3.5 Evaluation and validation of reference model

A high-resolution measuring network was used for the validation of the model by using 70 thermistor-based HOBO Pendant® temperature loggers (Gubler et al., 2020). The measurement lasted from May 16th to September 15th, 2018. A special requirement of these sensors is that they must be protected from direct sunlight. For this purpose, a custom-made radiation protection was developed which consisted of superimposing small melanin plates on each other. All technical details concerning the measurement data can be found in Gubler et al. (2020). The location of the sensors was chosen based on the maximum coverage of the spatial coverage with intersection from north to south and from east to west. Measurements were made at an interval of 10 minutes. The locations of the 70 measurement stations are shown in figure 3.7 below.

The results of the spatial temperature distributions of the reference model are presented in Table 3.2 and Appendix A. Simulation was done in one-hour intervals. The temperature contrast between the nearest simulation steps was insignificant. Therefore, the most contrasting time intervals (figure 4.1) have been selected for further analysis.

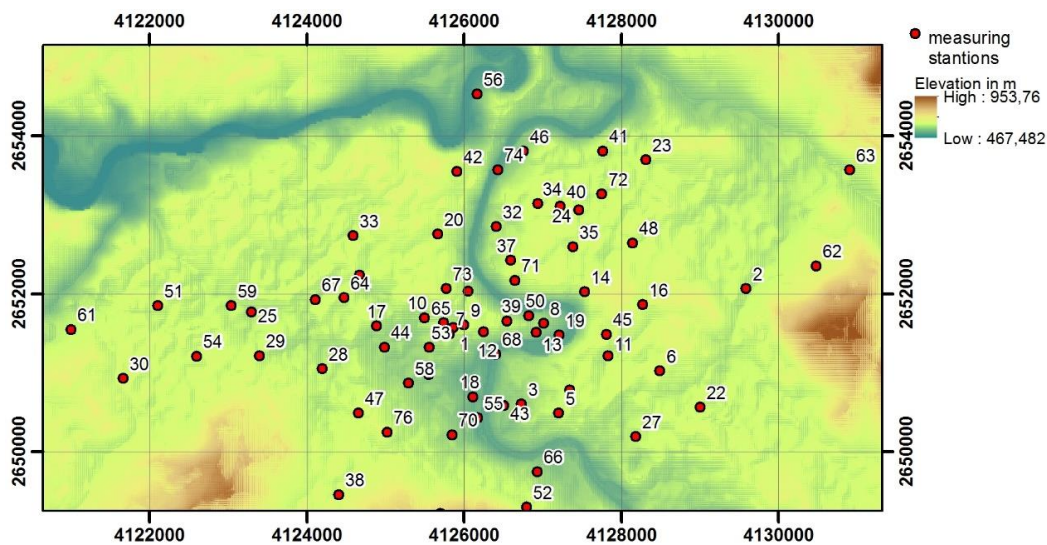


Figure 3.7: Location of the measurement stations for the model validation

The error of the model was determined by 70 stations of field measurements. Numbers on the chart are not in order because they correspond to the number of logs of the field measurements as per Gubler et al. (2020). The error is calculated as the difference between the simulation data and the field measurements data (figure 4.1). Instantaneous indicators (i.e. the temperature at 16:00) were used for the verification.

4 Results

Chart peaks dif_16 (16:00) were equal to receiving stations 4 and 65, which were located in areas of urban development with increased density (figure 4.1, 4.2). The peak shows that the temperature calculated by the model was 4-5°C above the temperature of the measurement station. Taking into account the results of the assessment, we can assume that MUKLIMO_3 has features with mean daytime temperature overestimation by 0.3°C on average, and mean nighttime temperature underestimation by 2.2°C on average.

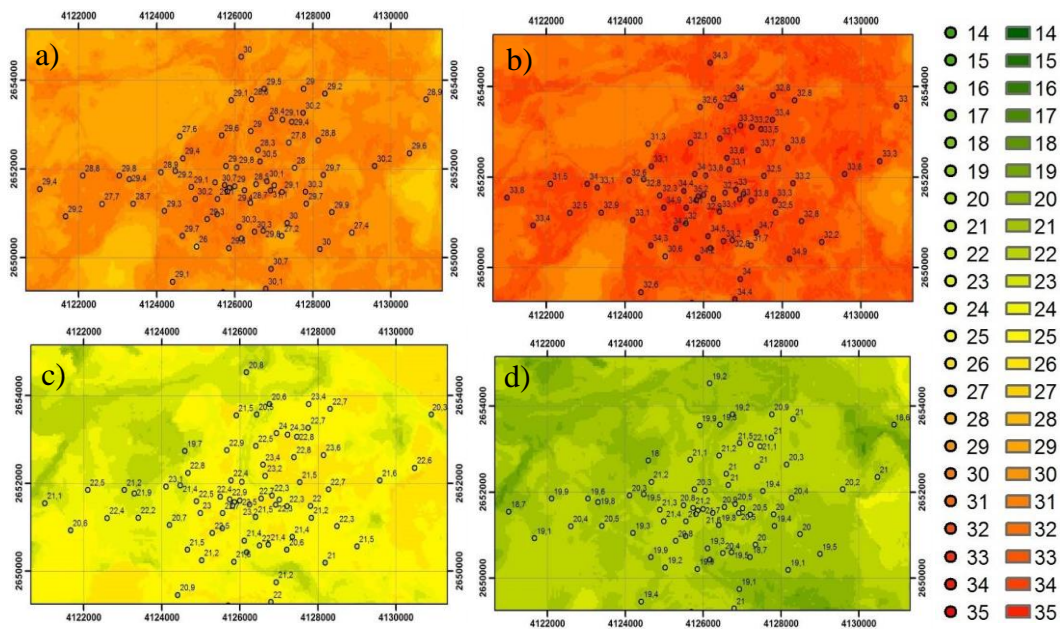


Figure 4.1: Temperature (in °C) in MUKLIMO_3 (colored area) and the measurement stations (filled circles) of August 3rd, 2018 at a)12:00, b)16:00, c)03:00 and d)07:00.

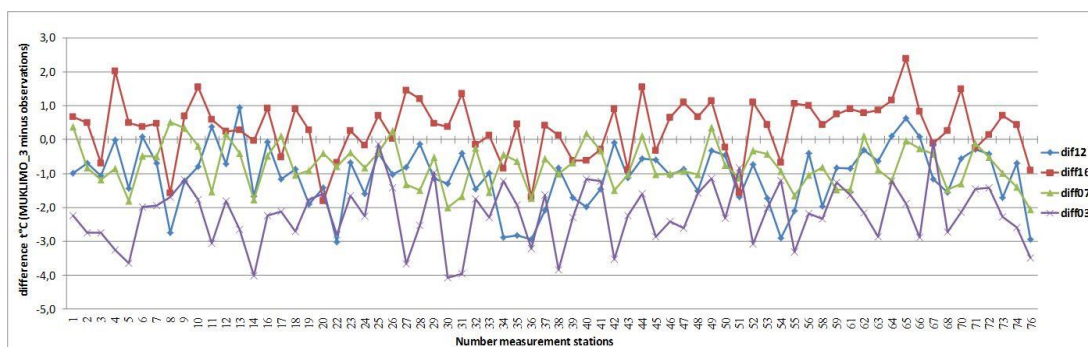


Figure 4.2: Temperature difference (MUKLIMO_3 minus measurement stations) at the location of the 70 low-cost sensors. Each number of logs corresponds of the field measurements by Gubler et al. (2020).

A station in the center of Bern was selected to monitor temperature changes during the day. The change of temperature within a day is shown in figure 4.3. The red line shows the temperature change of the model while blue shows the temperature of the measuring station in the city center. The figure shows that the model error changes during the day. At time points 1, 11, and 19 (9:00, 20:00, and 04:00 respectively), the error was at its maximum, within 4-6°C. At time points 8, 14, and 21 (17:00, 23:00, and 07:00 respectively), that error was minimal. At those points, the lines intersected and the error was near zero.

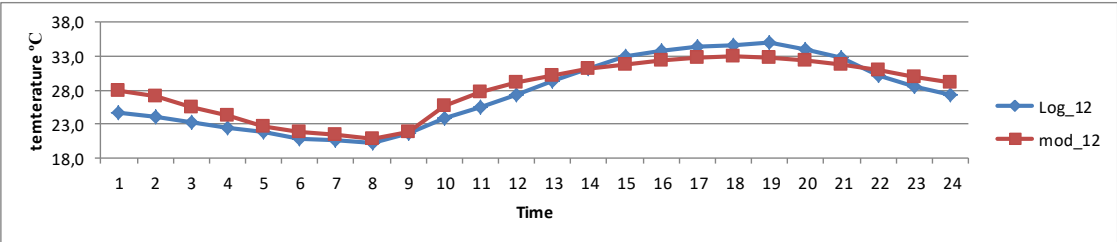


Figure 4.3: Day-time temperature (blue - measuring station 12) (red - reference model) at the corresponding grid cell in MUKLIMO_3)

The spatial change of temperature error between measurement stations and the simulated temperature is shown in the figure 4.4.

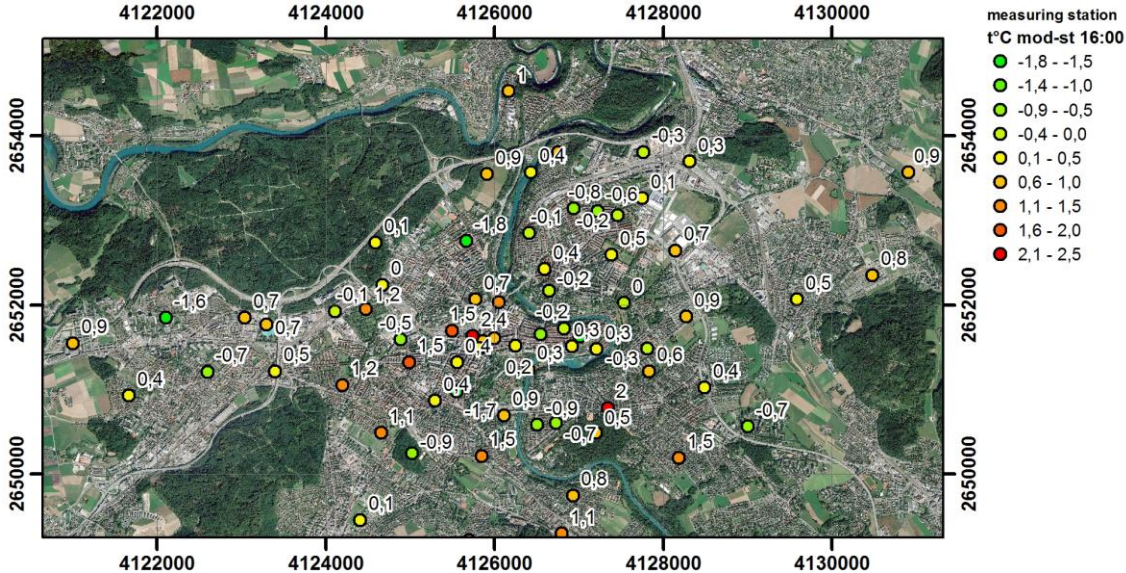


Figure 4.4: Location of the measuring stations for validation model and temperature difference between the simulated temperature and measurement stations at 16:00

Looking at figure 4.4, one can see green dots in the northwestern part of the city. This indicates that the model temperature is overvalued compared to ground measurements.

This may be due to the cooling effect of the forest in the northwest of the city. The red dots in a cent show that the model temperature was higher than the natural measurements.

A boxplot of the differences between the model and measured values is shown in figure 4.5. The blue point is the average. The horizontal line is the median. A negative/positive value means that the model shows colder/hotter values compared to the natural measurements.

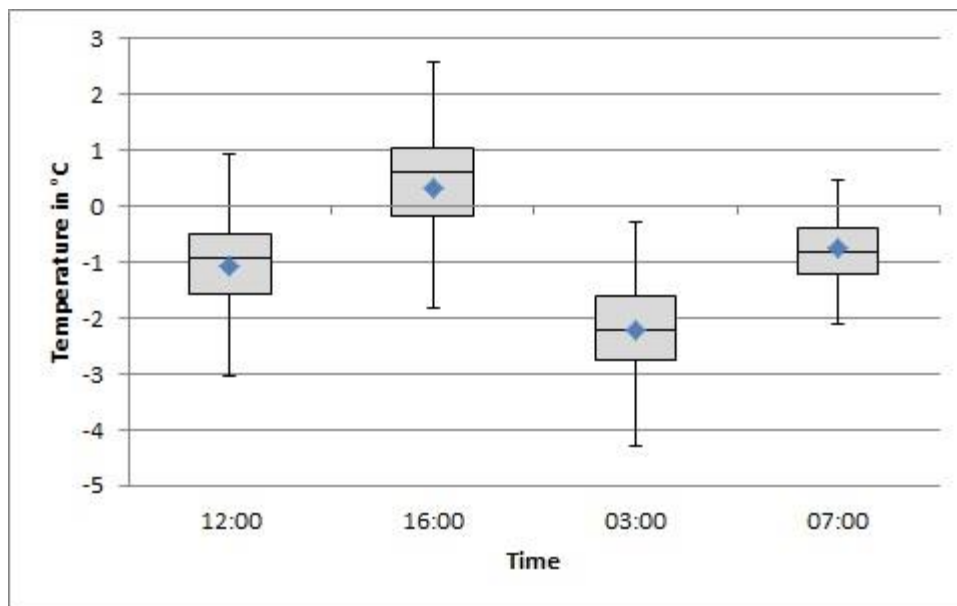


Figure 4.5: Boxplot of the differences between MUKLIMO_3 REF and the stations at all locations for 12:00, 16:00, 3:00, 7:00

Based on the validation results, the accuracy of modelling was calculated (figure 4.5). The daily average value was about -1°C and the standard deviation was about 0.8°C . For more information, see appendix C.

4.1 Analysis of reference model

By comparing the model results with measurements, one can see that the model data show a good result, similar in temperature to the control points. The greatest agreement can be seen at 16:00 and 07:00. The lowest agreement was at 03:00. While measurements show a decrease in temperature, the model had not yet had time to cool down. The highest temperature was reached at 16:00, which coincided with the natural measurements. The average temperature was -1°C at 12:00, $-0,5^{\circ}\text{C}$ at 16:00, $-2,2^{\circ}\text{C}$ at

03:00, and $-0,8^{\circ}\text{C}$ at 07:00. The daytime average was -0.2°C and the nighttime average was -1.5°C .

4.2 Modelled UHI of Bern

The UHI maps were constructed as the difference between the reference model and the temperature of the Zollikofen weather station at the time of modelling. As expected, the influence of temperature increase is intensively manifested in the urban area. The UHI map has the same error distribution as the reference map (figures 4.1 and 4.2).

The UHI maps (figure 4.6) show the intensity growth in the city center. The UHI peak in the city center was reached at 03:00 and was about 4.5°C .

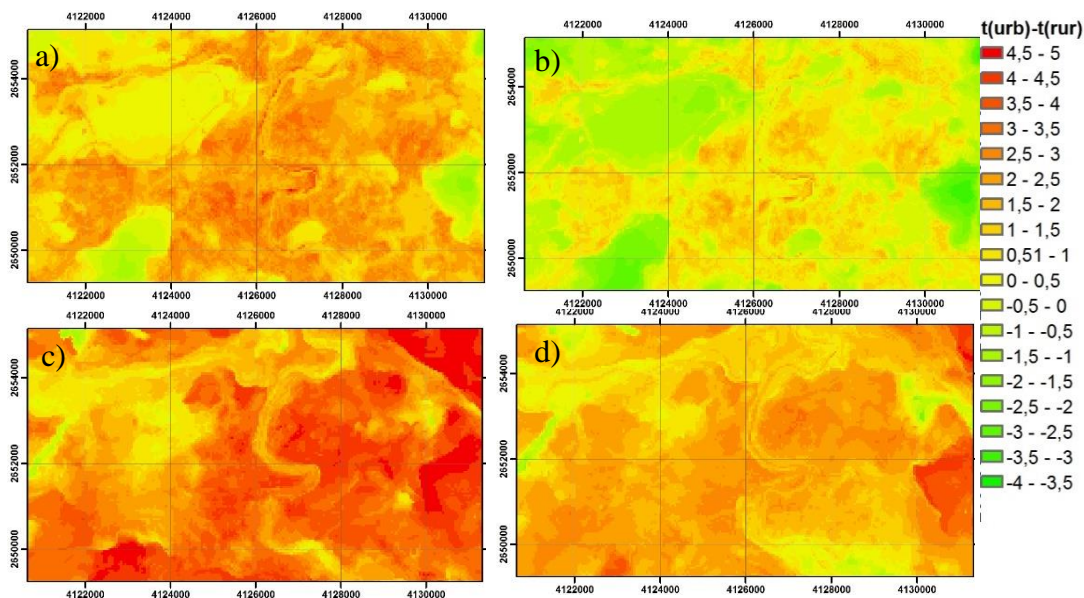


Figure 4.6: Urban Heat Island of Bern (REF minus temperature of the Zollikofen weather station at the time of modelling in each grid cell of the model)
a)12:00, b)16:00, c)03:00, d)07:00

There are the zones with increased building density, located in the north-east, center, and south-west parts of city (figure 4.6). In these areas, one can see an increase in UHI intensity. In figure 4.6a/b, the forest area in the eastern part of the city has temperatures $2-3^{\circ}\text{C}$ lower than the rural areas. This is due to both the features of land use classes and the relief. Forest areas cause a decrease in temperature of about 2°C , and the hills cause a decrease in temperature of about 1°C . In the nighttime, as seen in figure 4.6c/d, the hills have a temperature $4-5^{\circ}\text{C}$ higher than rural areas.

At night, the UHI is more homogenous. There are clearly built-up areas and the UHI is clearly traced on the hills. At 12:00 and 16:00, the green areas of the city, which have a cooling effect, are clearly visible.

At 07:00, one can see how the valleys in the west, southeast, and east parts of the city cool down. In the west of the city, the model displays the highway at 12:00 and 16:00 quite well. By 03:00 and 07:00, the borders are erased.

The largest temperature difference is at 07:00, where the temperature ranges from -3.16°C to 4.65°C .

To determine the spatial distribution of the UHI at night and in the daytime, a temperature profile of the line from the Bremgarten forest through the city center to the bottom of Dentenberg hill was built. The results show that the model highlights the green areas along the edges of the profile well. The UHI temperature was reduced in the Bremgarten forest by 1°C , and at the foothills of Mount Dentenberg by 2°C .

The temperature increased in the city center: the peak during the daytime increased by 2°C , and at night by 2.8°C . It means that the intensity of UHI at night is greater than the daytime. The graph clearly shows two drops in temperature. These are the effects of the Aara River and the relatively green neighborhood "Kirchenfeld" which is located near Egelsee. Figure 4.7 shows that the western sides of the mountains are intensely heated. According to Mathys et al. (1980), this temperature increase is the result of solar radiation exposure on the western sides of the mountains. Light energy has a maximum transmission when it falls to the ground at an angle near 90° . At sunset, when the city is already poorly heated, the sun's rays fall on the western slopes of the mountains at a perpendicular angle. As a result, the western slopes of the mountains heat up. Figure 4.6 clearly shows at 03:00 and 07:00 the residual heating of the mountains. These are the red areas in the east and south of the study area. At the same time, they are green at 12:00 and 16:00.

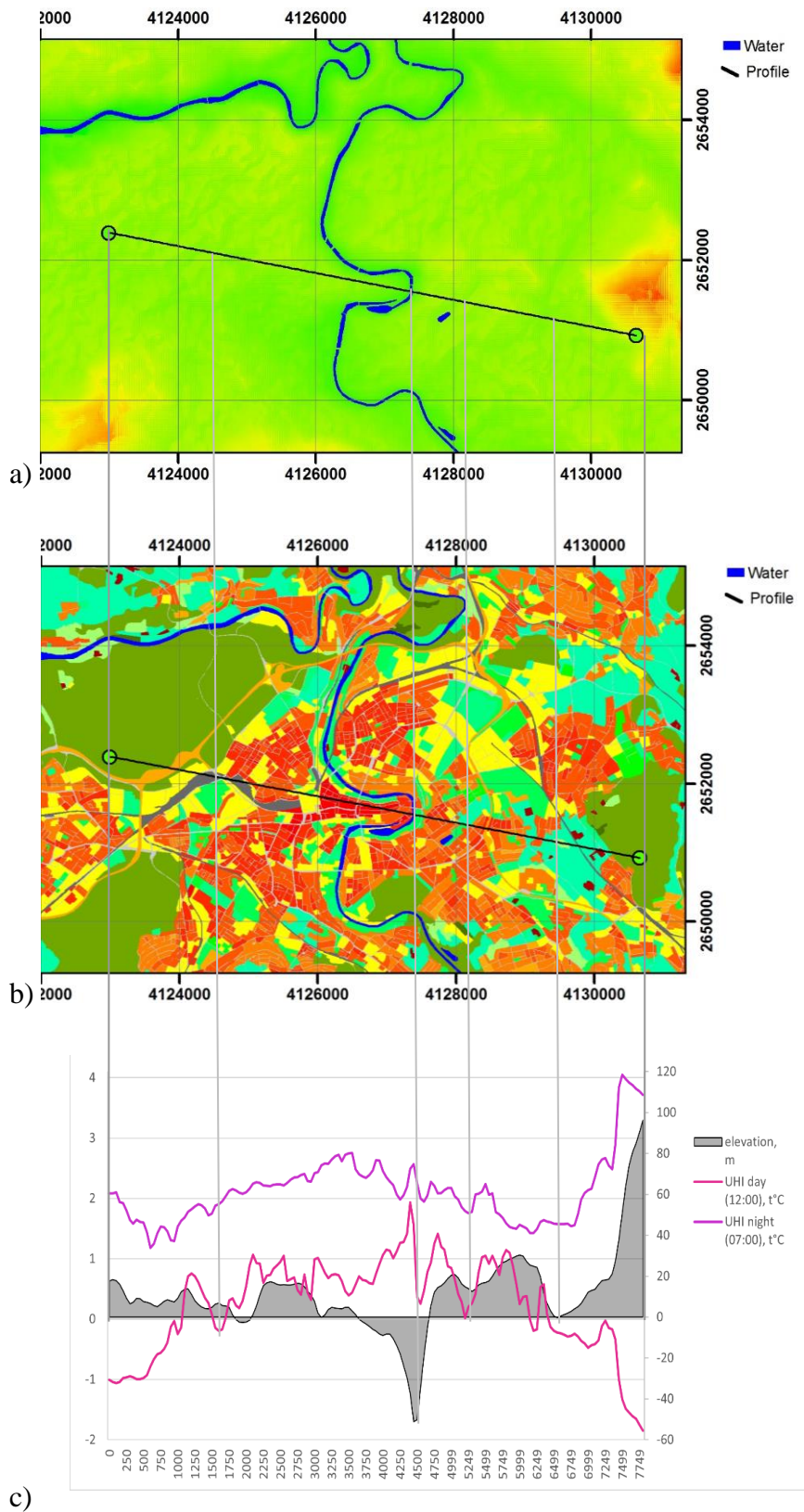


Figure 4.7: Urban Heat Island analysis profile from Bremgartenwald to Dentenberg, a) DEM, b) land use classes, c) day and night UHI

4.3 Evaluation of mitigation strategies

Mitigating strategies were analyzed by identifying differences when compared to the reference model. All received simulations were visualized in maps. The reference model calculated for August 3rd, 2018 the time points 12:00, 16:00, 03:00, 07:00. Figure 4.8 shows the difference between the calculation model and the reference model in absolute values, which are brought to a single temperature scale. This is done to facilitate comparison of results at all time points.

4.4 Surrogate climate scenario 2050

The RCP8.5 scenario of the projection CH2018 (NCCS, 2018) gives the average temperature on a global and regional scale. To get the spatial change of temperature on the city territory requires technology that includes land use and relief. In Muklimo_3, the calculated temperatures of RCP8.5 scenario have been introduced as initial data. For this purpose, the temperature in the model was raised by 4 °C. Other initial conditions have not changed. Muklimo_3 calculated the surrogate climate scenario 2050. To find the difference, the reference model temperatures were extracted from the temperature data of scenario 2050 (figure 4.8).

In the city center and its neighborhoods, temperature rose by 3.8°C. In the areas of parks and forests, temperatures increased by 3.5-3.6°C (figure 4.8a/b). At night, in the city center and its neighborhoods, temperatures increased by 3.6-4.5°C. In the areas of the Bremgarten forests, the temperature increases by 2.09°C (figure 4.8c/d). The average temperature increase in twenty-four hours was 3.8°C, except for some regions that were exposed to cold air (figure 4.9). The figure shows that within 24 hours, the average temperature changed non-linearly. During the day, it dropped from 3.8 to 3.7°C. At night, it rose from 3.8 to 3.9°C. It was indicated that the increase in temperature at night is greater than during the day.

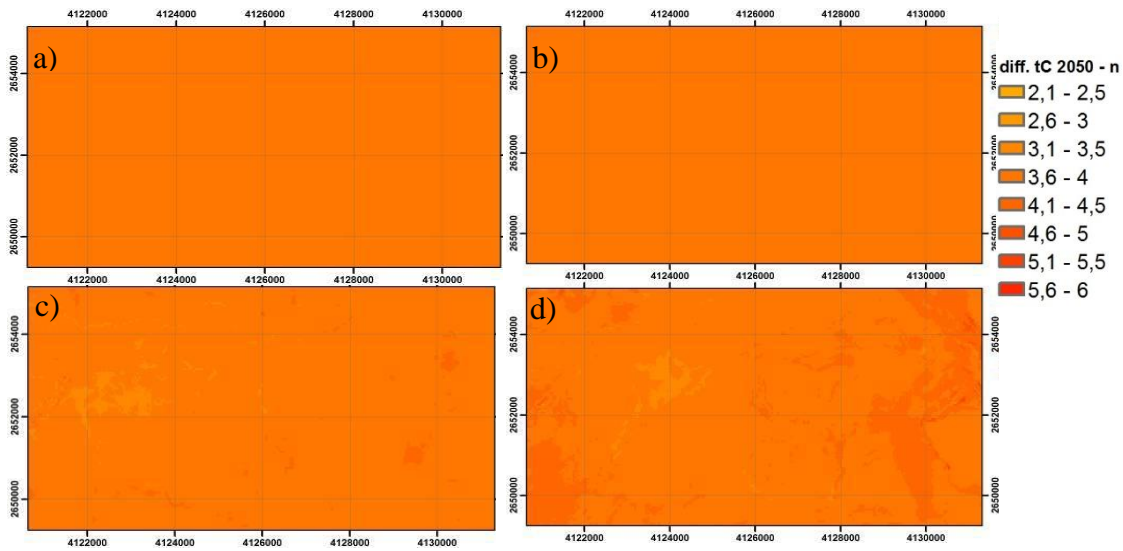


Figure 4.8: Temperature difference (in °C) between S2050 and REF; a) 12:00, b) 16:00, c) 03:00, d) 07:00.

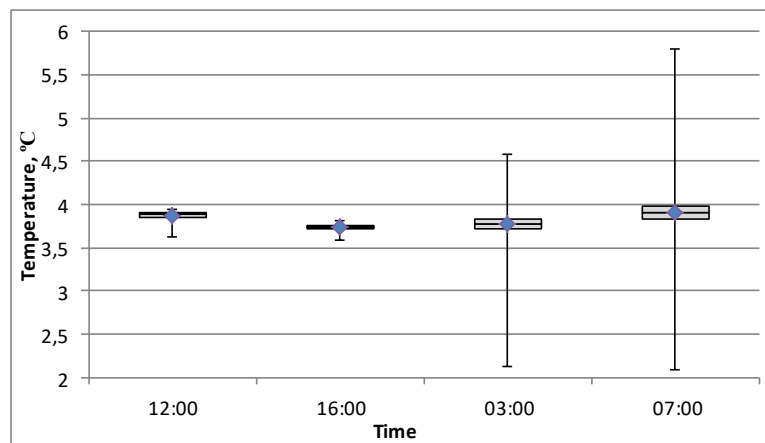


Figure 4.9: Boxplot of the differences between S2050 and REF locations for 12:00, 16:00, 03:00, 07:00

4.5 Sensitivity analysis

The main parameter of the model is temperature. The model is sensitive to some factors that impact temperature. Bern has a unique landscape: there are hills to the east and south and a lowland in the center. This forms temperature differences resulting in a pressure difference and wind. The river flows through the city center from the south to the east. It forms an air corridor for regional and global air mass movements. Simulation of two wind directions (SW & NE) was performed. It evaluated the temperature change under the influence of the northeast wind. During the day, the temperature difference

between northeast and southwest was allocated evenly across the study area. (figure 4.10a/b). The daytime temperature (figures 4.10a/b and 4.11) ranged from -1 to 1°C, and 50% of all temperatures varied between from -0.3 to 0.2°C. The effect of wind during the day was near zero. At night, the range increased from -4.8 to 7°C, and 50% of all temperatures varied between from -1 to 1°C (figure 4.10c/d, 4.11). Figure 4.10d shows the effect of forest cooling in the south-west of the city (green area) At night, there was also a heat effect (seen in the red and orange areas) from the western side of the hills in the southeast and southwest of the area. Wind speed affected the transfer of cold and hot air in the wind direction. Figure 4.10a/b shows the shift of cool air from the forest (green area) for about 1 km.

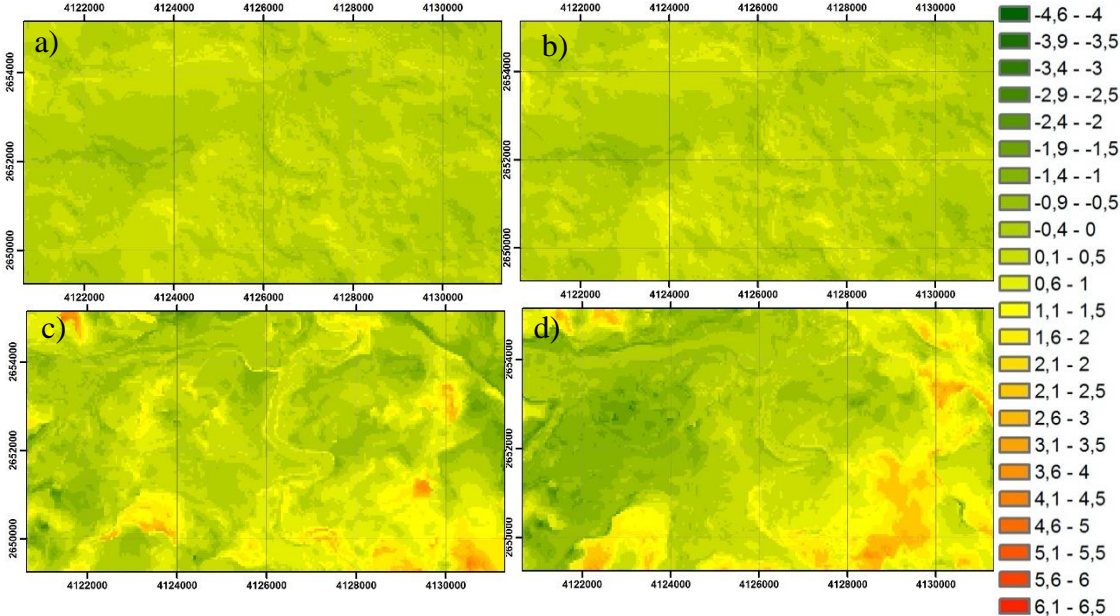


Figure 4.10: Temperature difference (in °C) between WDF and REF a)12:00, b)16:00, c)03:00, d)07:00.

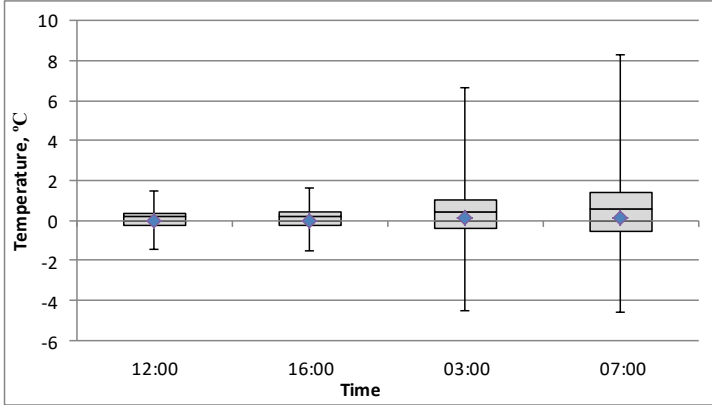


Figure 4.11: Boxplot of the differences between WDF and REF locations for 12:00, 16:00, 03:00, 07:00

Muklimo_3 simulates the temperature from its minimum to its maximum. During the day, this temperature changes depending on this difference. Also, the Navier–Stokes equations emulate air turbulence. The more time it takes to simulate the effects, the more visible it is. To evaluate the sensitivity of temperatures from the time of modelling, S2D is done. Simulation time increased to two days. Figures 4.12 and 4.13 show that the temperature change fluctuated around zero with a range of $\pm 0.5^{\circ}\text{C}$ during the course of 24 hours. In the forest area, the temperature decreases up to -1°C on average. Only at 12:00 was there a cooling effect from the forest (figure 4.12a).

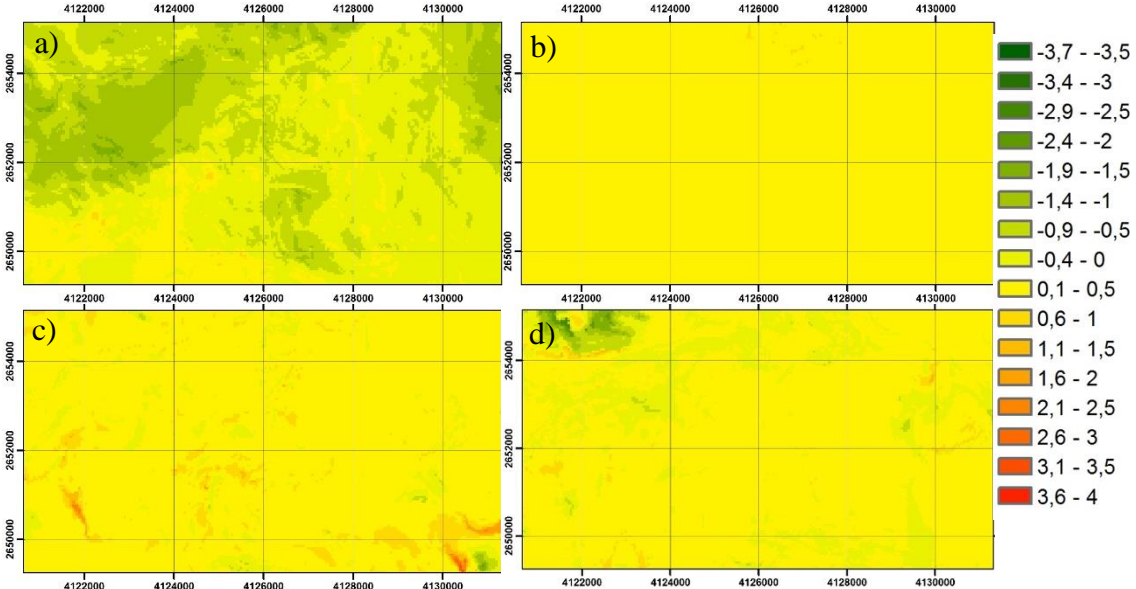


Figure 4.12. The difference between the first REF (August 3rd, 2018) and the second S2D day (August 4th, 2018) a) 12:00, b) 16:00, c) 03:00, d) 07:00.

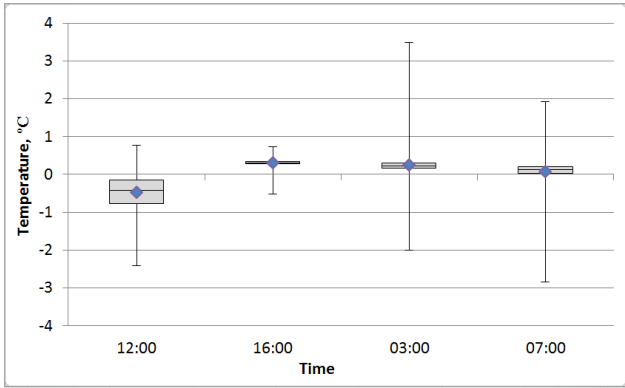


Figure 4.13: Boxplot of the differences between S2D and REF locations for 12:00, 16:00, 03:00, 07:00

4.6 Mitigation strategies of modelling

The spatial distribution of temperature differences will be shown to gain an understanding of the impact of different mitigation strategies on the entire simulation domain.

4.6.1 Green mitigation strategy

The 6% increase in the green area in the study area with forests led to a marked decrease in temperature in the central areas of the city. During the daytime, the average temperature decreased by 2.5°C (green area of figure 4.14a/b). At night, in the same areas, the temperature dropped by more than 3°C (figure 4.14c/d). On average, in the study area, the temperature decreased by -0.5°C (figure 4.15).

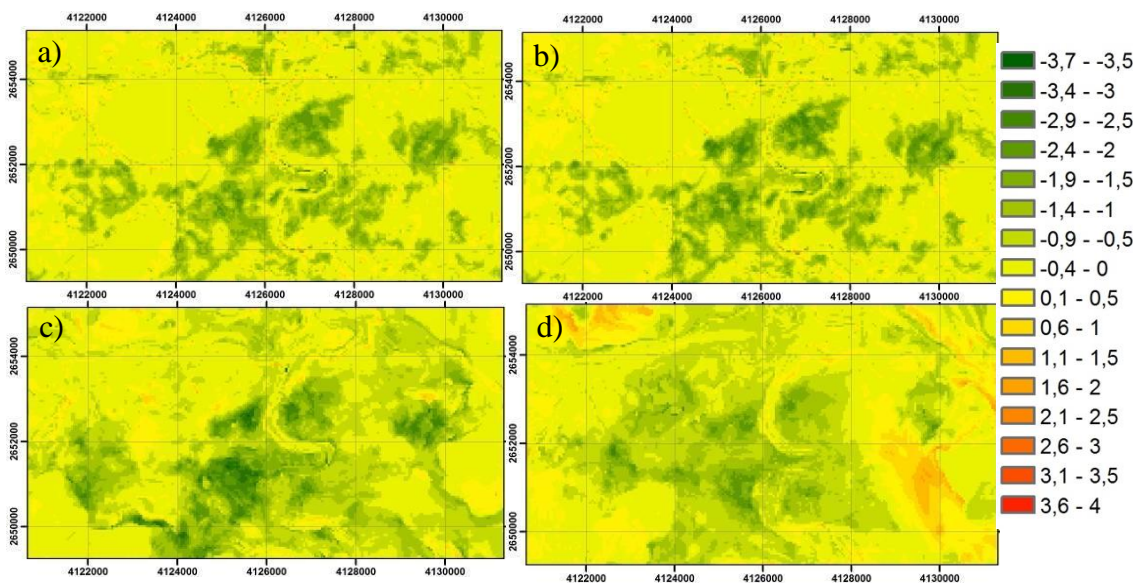


Figure 4.14: Temperature difference (in °C) between RG (increase the forest area by 6%) and REF; a) 12:00, b) 16:00, c) 03:00, d) 07:00.

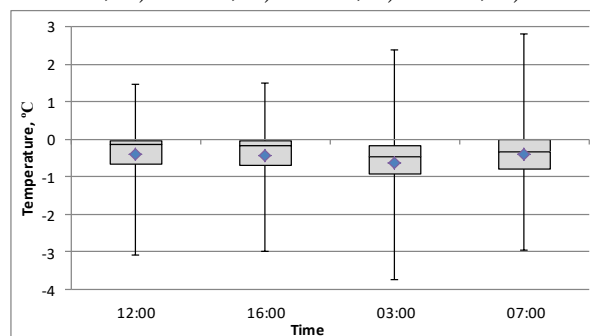


Figure 4.15: Boxplot of the differences between GR and REF locations for 12:00, 16:00, 03:00, 07:00

Two extreme models were simulated. Maximum decrease in temperature was achievable with idealized development of green building strategies. The cooling properties of this model were expected to be comparable with those of the forest. The industrial areas were replaced by forests (classes from 1 to 7, figure 3.5). The area of the forests in the total study area were increased by 54%. The second extreme model was modelled based on the hypothesis that forest land is lost during cutting or emergency situations. The "forest" class was replaced by the 7th class called "Industrial, commercial, public, military and private units".

Where urban areas were replaced by forests (areas of development), there was a decrease in temperature by 5°C during the day (green areas of figure 4.16a/b). At night, in the central areas, the maximum temperature reduction was up to 6°C (figure 4.16c). At 7:00, the cooling effect from the forest was reduced by 2°C (figure 4.16d).

Increasing the "forest" land use class by 54% allowed for an average temperature reduction of 2-3°C in the daytime and a 2.5-3.5°C temperature reduction at night (figure 4.17).

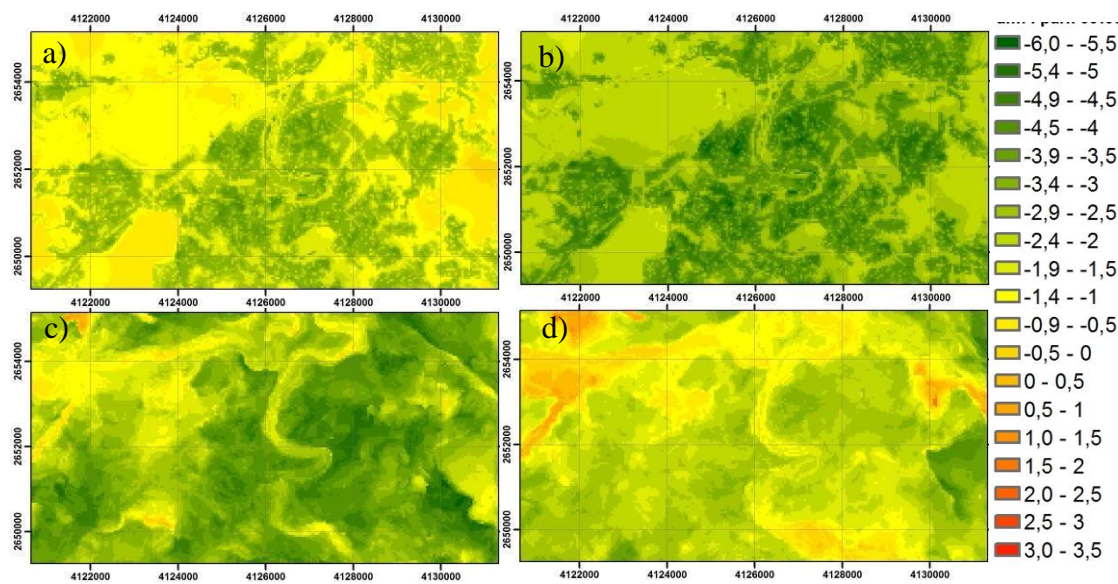


Figure 4.16: Temperature difference (in °C) between IGR (increase the forest area by 54%) and REF; a) 12:00, b) 16:00, c) 03:00, d) 07:00.

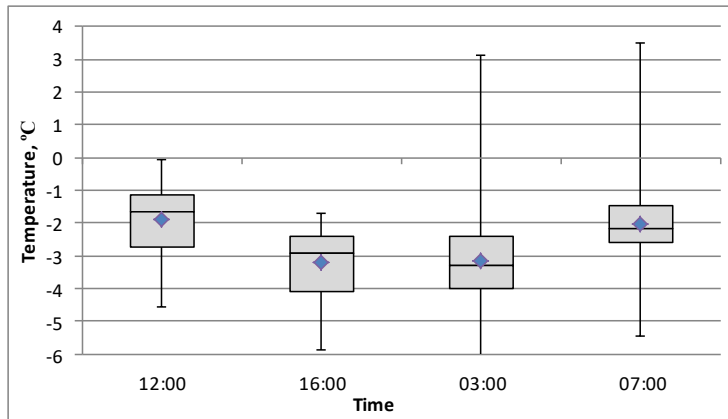


Figure 4.17: Boxplot of the differences between IGR and REF locations for 12:00, 16:00, 03:00, 07:00

During the day, ex-forest areas (orange areas in figure 4.18a/b) have a temperature increase of 3°C. In the center and neighborhoods, the picture did not change during the day. At night, ex-forest areas (red and orange areas figure 4.18c/d) have a temperature increase of 4-5°C. The contours of the ex-forest are more washed out at night (figure 4.18c) than in the daytime (figure 4.18a). This is due to the Navier–Stokes equations and the wind shift. Figure 4.19 shows an average temperature increase by 1.5°C in the study area over the course of 24 hours. The daytime average was 0.5°C, and the nighttime average was 1.7°C.

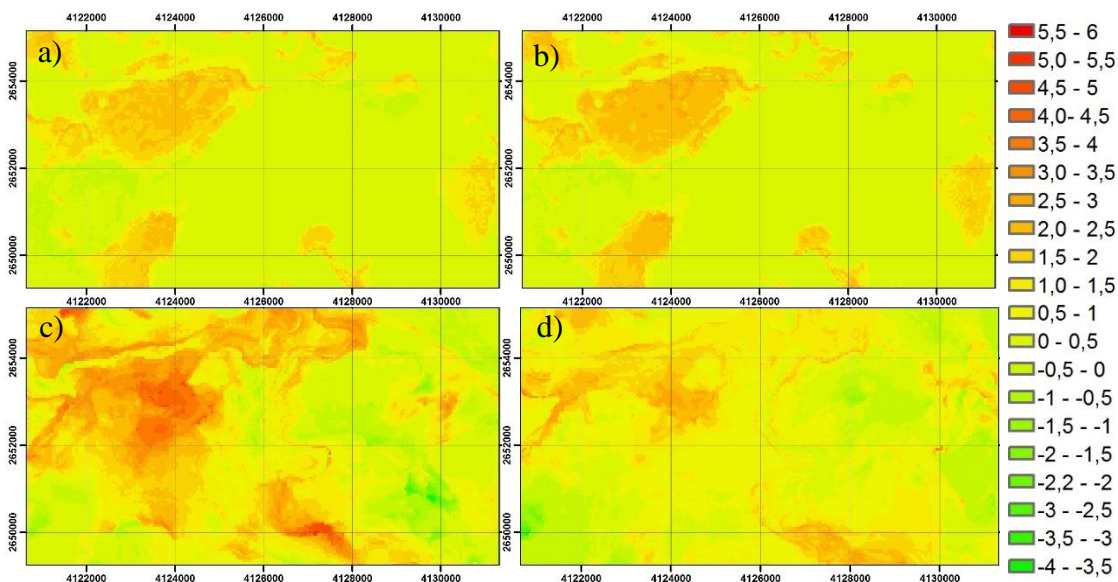


Figure 4.18: Temperature difference (in °C) between NOGR and REF a) 12:00, b) 16:00, c) 03:00, d) 07:00.

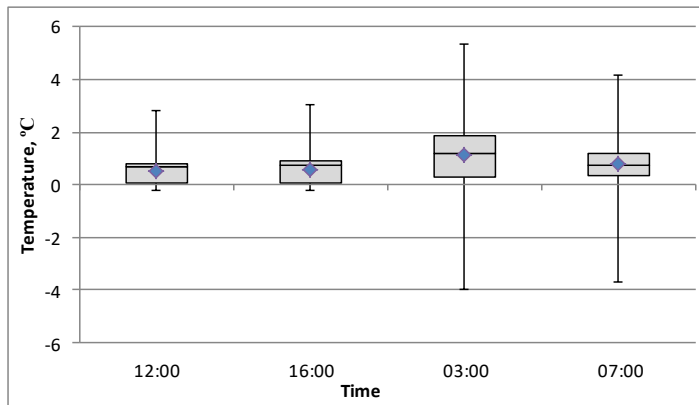


Figure 4.19: Boxplot of the differences between NOGR and REF locations for 12:00, 16:00, 03:00, 07:00

4.6.2 White mitigation strategy

The albedo level was increased to 0.7 in built-up areas and to 0.5 in roads. Temperatures decreased by 0.25-0.5°C during the day in the areas where the albedo was changed (green areas figure 4.20a/b); that is about 0.12-0.25°C per 0.1 albedo. A decrease in temperature at night was not observed as the increase in reflective properties of materials only works during the day (figure 4.20c/d). During the day, the model shows an average temperature decrease of 0.1°C. (figure 4.21). At night, the average temperature did not change. At night, the temperature dispersion increased due to fluctuations in the zones of extreme parameter changes (foothills, river valley, forest border) (figure 4.21 at 07:00).

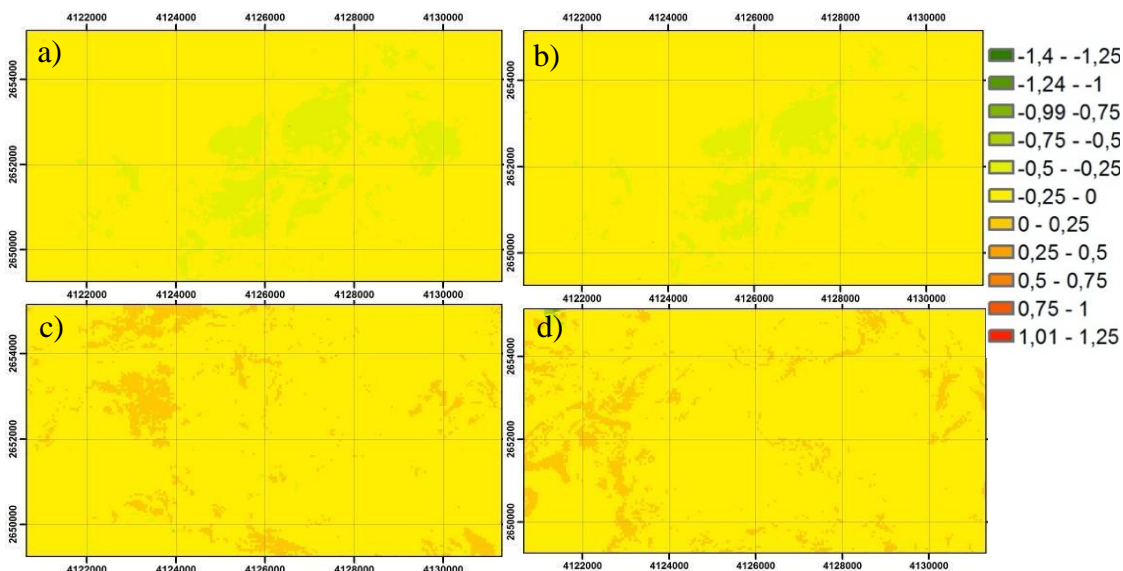


Figure 4.20: Temperature difference (in °C) between ALB (increase albedo up to 0.5-0.7) and REF; a) 12:00, b) 16:00, c) 03:00, d) 07:00.

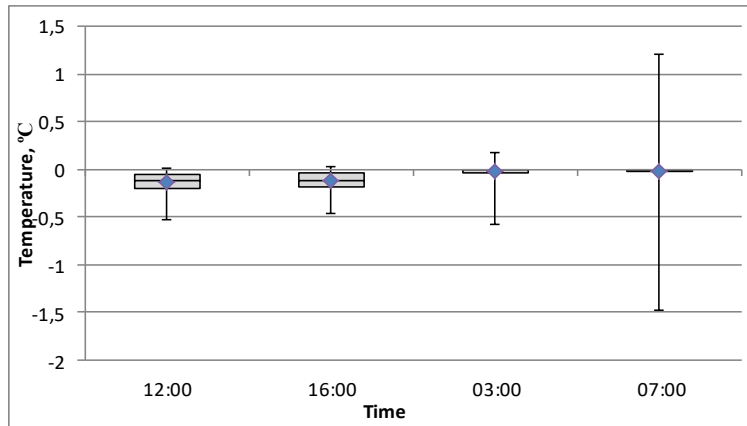


Figure 4.21: Boxplot of the differences between ALB and REF locations for 12:00, 16:00, 3:00, 7:00

4.6.3 Blue mitigation strategy

The blue strategy allows lowering of temperatures only locally. The model shows temperature reduction only in places where a new land use class "water" has been added. In these places, the daytime temperature decreased by 1.5°C on average. Figure 4.22 shows water bodies are heat accumulators. During the day, green is a sign of a temperature drop of 2.5°C in water bodies (figure 4.22a/b). At night, red areas showed an average temperature increase of 3°C at the bodies of water (figure 4.22c/d). On average, temperature change was near to zero during the course 24 hours in the study area (figure 4.23)

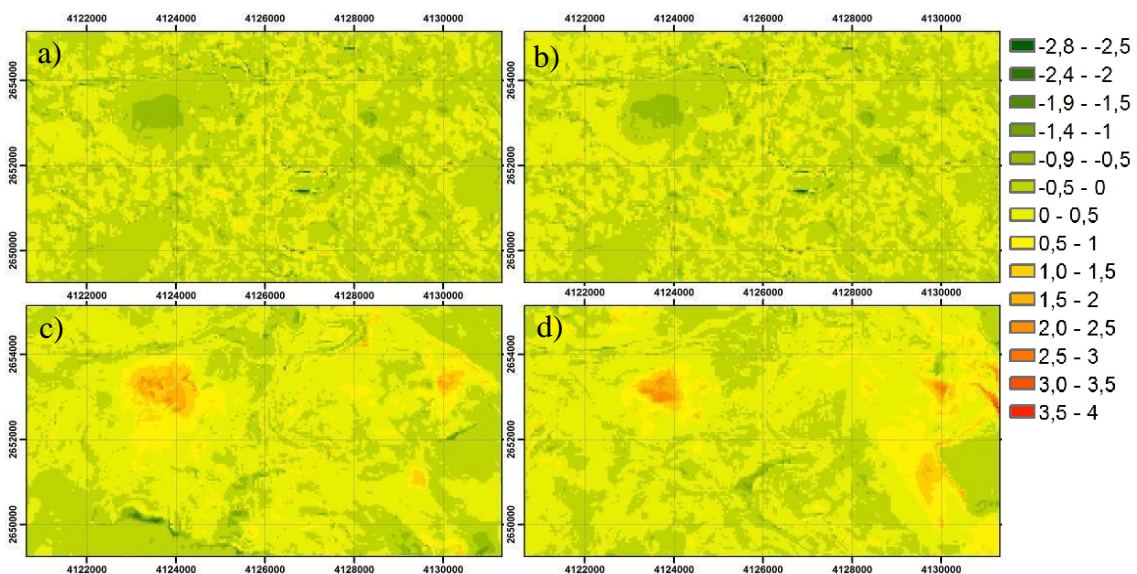


Figure 4.22: Temperature difference (in °C) between BL (increase water body by 3.8%) and REF a) 12:00, b) 16:00, c) 03:00, d) 07:00.

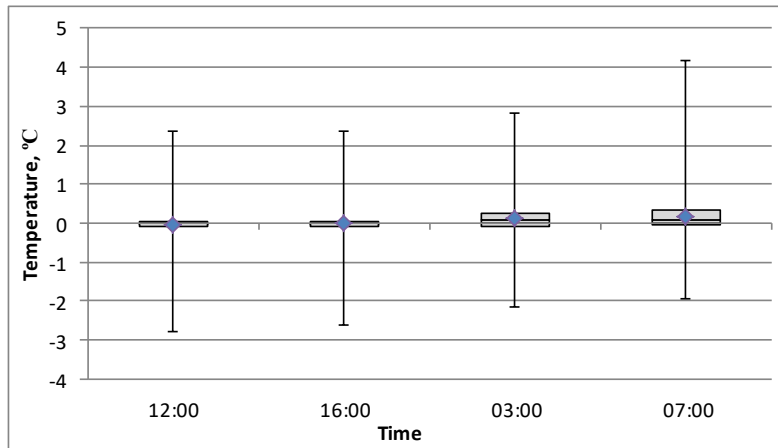


Figure 4.23: Boxplot of the differences between BL and REF locations for 12:00, 16:00, 3:00, 7:00

4.6.4 Simulation of green chantiers

The application of the model shows the local impact in places where the *chantiers* were replaced by the "urban green space" land use class. On average, the decrease in temperature in these places reached about 2°C during the course of 24 hours (figure 4.24). The maximum temperature reducing in is up to 3°C locally. In this case, small, local green areas evenly located throughout the city affected the overall temperature of the city. On average, temperature change was near to zero during the course of 24 hours in the whole study area (figure 4.25)

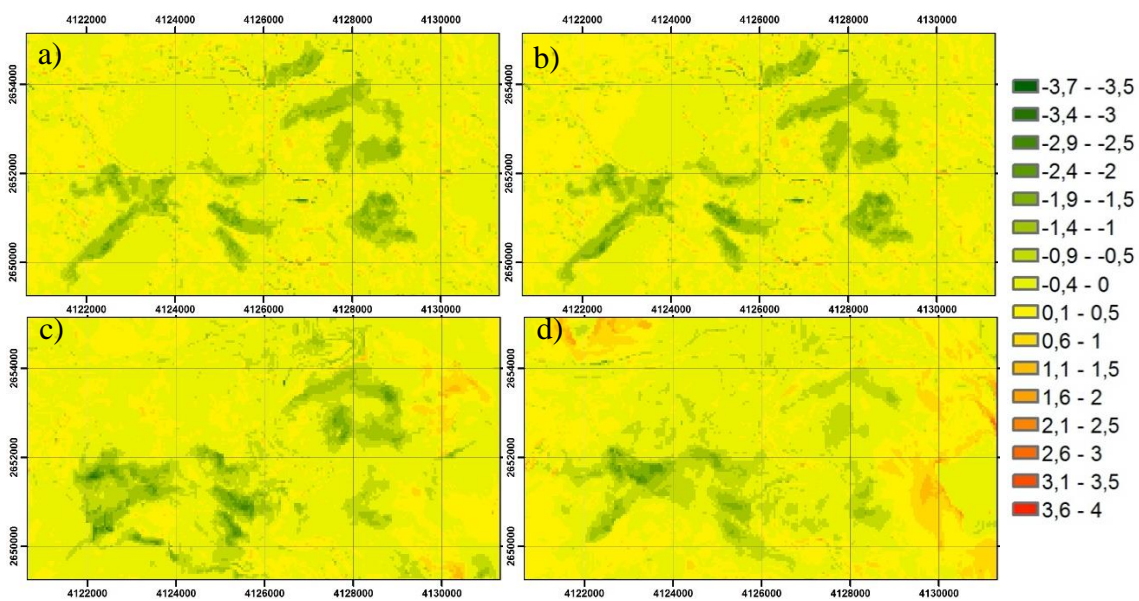


Figure 4.24 Temperature difference (in °C) between CH and REF; a) 12:00, b) 16:00, c) 03:00, d) 07:00.

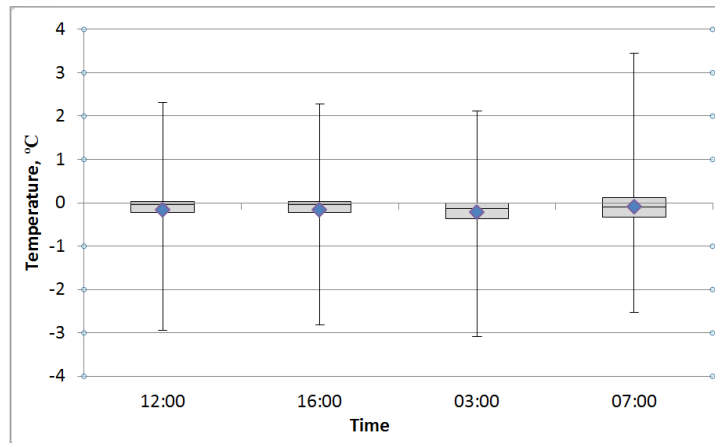


Figure 4.25: Boxplot of the differences between SCH and REF locations for 12:00, 16:00, 3:00, 7:00

4.6.5 Implementation in urban development

The result of the UHI was overlaid on the land use map. The most thermally problematic *chantiers* were obtained as a result of crossing them with the UHI. Figure 4.26 shows that the northeastern part of the Eigerstrasse corridor was most influenced by the UHI. The general situation in terms of the influence of UHI on Bern can be estimated from Appendix C.

Modelling results showed that UHI intensity was most pronounced within and around the city center. As one can see, the *chantier* of the Eigerstrasse corridor falls completely in the epicenter of the UHI (figure 4.26). The urban development of the city of Bern, in accordance with the STEK 2016 concept, plans to increase the density of the buildings, which could change of the air mass flow and additional heat storage (Stadt Bern, 2017). This should be taken into account when planning the development of the city in general and the *chantiers* in particular.

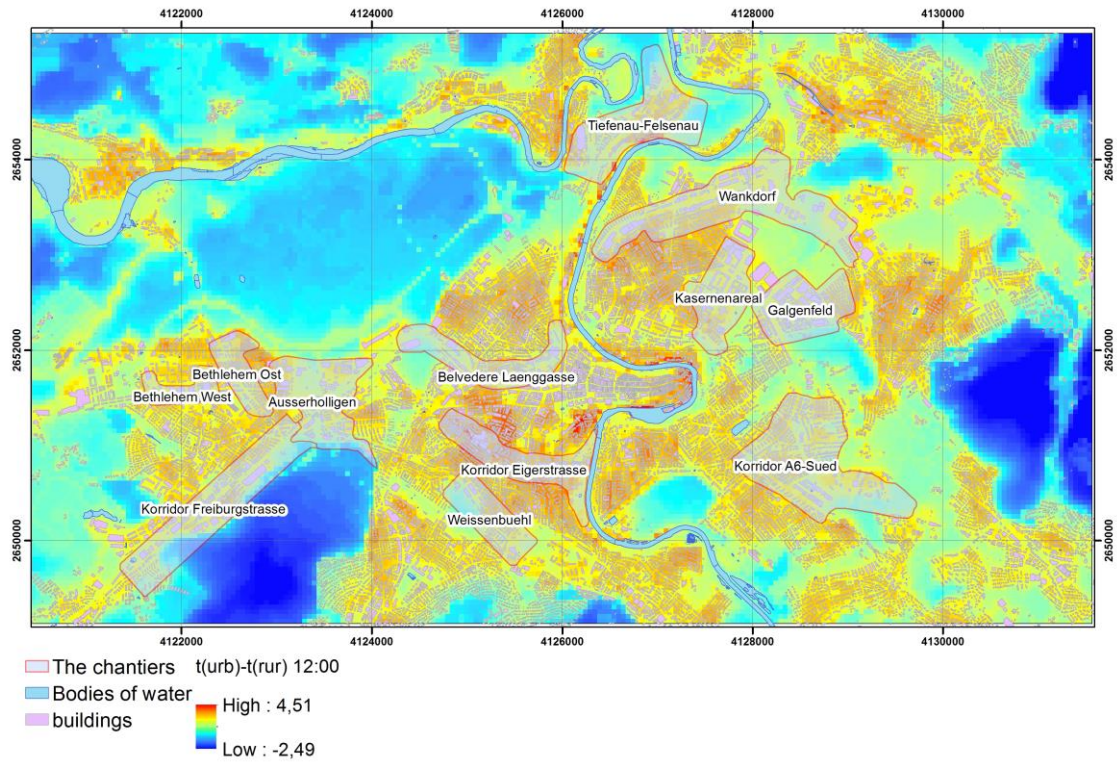


Figure 4.26: Result maps: chantier contours superimposed on grid UHI at 12:00

5 Discussion

Initial temperatures

Input meteorological data for the model can be taken from both the weather station (Zollikofen) and the model itself. The measuring station might be located both inside and outside the model range. It is important that this station sufficiently describes the climate around the city, without being affected by construction work, i.e. urban heat. Input temperatures from the weather station were corrected because the model produced an underestimated temperature at the initial calculations. The increase in initial temperature by 2 allowed to improve the average error from -2°C to 0°C in the daytime, and from -4°C to -2°C at night. This may be due to the installation of measuring stations in areas with low ventilation and the presence of a protective hood, which accumulates heat and produces excessive temperature. There is a regularity of spatial error distribution (Figure 4.4). There are also high errors at the edge of transition classes forest - urban area. When building a pixel of $50\text{m} \times 50\text{m}$ the values of land use classes are averaged. It may happen that the station is set on one class (e.g., urban area) and the model has averaged and chosen another class (forest) therefore there are inconsistencies. The recommendation is to select stations with the area around which is comparable to the area of a pixel. Also one should critically consider the stations that are on the borders of transition from one class to another.

Effect of terrain

The model has not given expected cooling effect of the Aare river. This is caused by the 50 m resolution chosen for this research, meaning the grid cell is wider than the river.

The western slopes are heated in the evening and affect the UHI at night. The northern slopes are less heated. On the maps (Fig. 4.6c/d; 4.8c/d; 4.10c/d etc) you can see the red spots which are located mainly east and southwest where the hills are. In the south, the steep right bank of the Aare river valley can be seen (Figure 4.19c).

In the daytime, on the contrary, these places reduce the intensity of the UHI. There are forests on the slopes and the presence of moisture and vegetation in the river valley. (Figure 4.6b).

Influence of the sky view factor

The effect of heating similar to that of the western slopes of the hills should be observed in the city. The western sides of the houses should heat more and affect the UHI at night. However, the selected resolution is much larger than a single house and the effect is not visually observed. The open sky factor should theoretically impact UHI formation too however the selected resolution smoothers this effect.

The temperature difference during the day and night

Calculated UHI intensity maps show the difference between day and night time (Fig.4.2, 4.6). At night, an urban heat island is formed above the city. It has a vast area and swirls (red spots in Fig. 4.6c; 4.8d; 4.19c). During the day, the thermal island is more diverse and is characterized by the influence of smaller elements (building blocks, roads, etc.). The hottest areas are located in the city centre, the southern neighbourhood of the centre and the north-eastern neighbourhood of the centre (Figure 4.6a). The most important features of the city's day maps are forested areas and hills in the south and east (green areas shown in Chart 4.6b). At night, water bodies and western hillsides are the most important factors of heating (figure 4.6c; 4.10d; 4.23d).

Model launch

The model disadvantages include the following: no pollution data, no real time data, extensive temporal and software resources needed to obtain the result. To make calculations for one day at 1hour interval, 30 hours should be spent for the cluster of 24 modern computers. For the purpose of the model adaptation for the specifics of Bern, the model was calculated more than 20 times. The same was necessary to identify the impact of these or those parameters on the different strategies.

Mitigation strategies

As in the existing studies (O'Malley et al., 2015), the green strategy showed a greater decrease in temperature. In green strategy 6% of the city area was replaced by forests with tree height of 20 meters and leaf area index of 1.5, in green Chantiers strategy 12% of the area was replaced by green urban areas (parks) with tree height of 10 meters and

leaf area index of 0.9. The model showed the same temperature decrease in places of implementation even though arable land (annual crops) not concentrated in the city centre was replaced by forests, and built-up areas were predominantly concentrated in the city centre. Thus, we can assume that the location where the strategy is implemented and its application in the peak points of UHI play an important role in overall strategy efficiency. That means, as in the study of Žuvela-Aloise et al. (2018), that the application of mitigation strategies even with initially less cooling effect in the center of the city, i.e. at the epicenter points of the UHI, will play a more significant role than potentially more effective strategies, but at the edge of the city.

The white strategy showed a local temperature drop of about 0.5 C during the day, which is similar to the studies of Santamouris (2014) and to Žuvela-Aloise et al. (2018). At night, the model warmed up irregularly small areas in the simulation area at about the same temperature. This may be due to the fact that the model uses the Navier-Stokes equations to model atmospheric flows, i.e., the model creates vortexes based on the temperature values of air inside the study area and regional air mass transfer is not evaluated and not considered.

The blue strategy showed a temperature decrease of ca. 2.5°C at the application sites, which is comparable to the study of Volker et al. (2013), but warmed them up at night as in the studies of Theeuwes et al. (2013) and Zuvela-Aloise et al. (2016). It may occur because the water temperature is constant (18°C in this study) and there is no flow velocity parameter in the model, which has influence on this cooling effect.

Overall all the strategies show better results only in places where they are implemented, so to get a better cooling effect, all of them should be applied over large areas (the same is shown in Kubota et al.(2017), Zuvela-Aloise et al.(2016).

6 Conclusion

The implementation of the urban climate model to the city of Bern was held for the first time and was successfully adapted. The accuracy of the reference model was estimated. The mean value during the day is -0.5°C and at night is -1.5°C . The standard deviation is less than 0.9°C day and night. It overestimates peak temperatures during the day and understates them at night and has better coincidence with field measurements during the day. We can conclude that the daytime error of the Muklimo_3 model is less than the nighttime error. This is due to Muklimo_3 not including the thermal energy produced by the city itself, but only the energy from solar heating. The night field measurements include both the components of accumulated solar energy and the city's own energy. But the night model measurements are only components of the accumulated solar energy.

The model has not shown the expected cooling effect of the Aare river. The reason is the 50 m resolution chosen for this research, wherein the grid cell is wider than the river.

The UHI intensity was calculated as the difference between the validated data of the reference model and the Zollikofen weather station. The validation was performed with a wide network of field measurements from 70 observations within the city while the Zollikofen weather station presented the rural air temperature data. The peak of the UHI increased at night and reached 2.8°C in the city center. The average UHI intensity was $1\text{-}2^{\circ}\text{C}$ during the day and $2\text{-}3^{\circ}\text{C}$ at night. These results were comparable with the research of Burger (2020) based on LUR models. The data from the profile which was conducted from Bremgarten forest through the city center to the bottom of Dentenberg Hill, confirmed Oke's 1982 hypothesis that the intensity of the UHI at night is greater and smoother than at the daytime.

The simulation of the white, blue, and green mitigation strategies has shown the different cooling effects dependent on the time of the day and of spatial distribution. The white strategy has the potential to reduce the daily temperature up to 2°C . An increase in albedo by 0.1 leads to a daytime temperature decrease by 0.14°C , which is comparable to Santamouris (2014). A decrease of the temperature by $0.5\text{-}0.7^{\circ}\text{C}$ in the

places of implementation and 0.5°C on average matches the research in Vienna (Žuvela-Aloise et al., 2018). The blue strategy shows on average a 0.2°C decrease, but can locally reduce the daily temperature in places up to 2.5°C, the same as Völker et al. (2013). That may be underestimated, however, because the water temperature was constant (18°C in this research) and there was no flow velocity parameter in the model, which has influence on the cooling effect. While the blue strategy decreases the temperature only during the day and heats the bodies of water at night, the cooling effect from the green strategy is throughout the day. The green strategy causes on average a 1°C reduction of the temperature in the whole study area, but up to 3°C in the built-up areas in the city. This is in accordance with Rodatz's research (2012). Thus, the green mitigation strategy is the most acceptable in the task of reducing temperatures.

We can assume that the model results are suitable for urban planning. The model shows good results on the urban and neighborhood scales. For buildings of scale, it is necessary to increase the resolution. It is important to note that each city has its own UHI features. To sum up, we were able to prove that all of the selected strategies do have an impact (some more limited than others) on the UHI. The Muklimo_3 shows the greatest effect on temperature reduction in Bern via the green strategy. However, to achieve a significant reduction of UHI intensity on an urban scale, it should be widely applied due to very limited available space in the urban landscape. It should be noted that this strategy requires time and money for adaptation, growth, and maintenance. Moreover, the city center of Bern is a UNESCO Heritage Site, which is the limiting factor for the implementation of mitigation strategies. Nevertheless, the results of the modelling provide the knowledge of Bern's UHI intensity, its diurnal and spatial variability, and its topography specifics, which should be considered when assessing the viability of UHI mitigation strategies in the city.

Acknowledgments

Firstly, I would like to thank my supervisor Prof. Dr. Stefan Brönnimann and my advisor Moritz Gubler. They have patiently led me through my research path, have always had spare time to discuss various issues and problems and have always been able to come up with advice. Secondly, I would like to thank ZAMG research community and especially Maja-Zuvela Aloise and Brigitta Hollosi for their help and support with MUKLIMO_3 model and sharing valuable data. Next, I would like to thank Andrey Martynov, who helped me with IT support and without whom I wouldn't have been able to run the model quickly. Furthermore, I would like to thank Andreas Heinemann for being always there to help and for providing me ArcGIS data. I would also like to thank the whole Meteotest team and especially René Cattin and Jan Remund for various ideas and interest towards my research. I would like to thank my dear husband Dmitrij Antonow who has always supported me with such a valuable resource as time and inspiration. Finally, I would like to thank Anna Kulakovskaya, Dominik Vogt and Angela-Maria Burgdorf for their help and share their valuable opinion.

References

- Aflaki, A., Mirnezhad, M., Ghaffarianhoseini, A., Ghaffarianhoseini, A., Omrany, H., Wang, Z., & Akbari, H. (2017). Urban heat island mitigation strategies: A state-of-the-art review on Kuala Lumpur, Singapore and Hong Kong. *Cities*, 62, 131–145. <https://doi.org/10.1016/j.cities.2016.09.003>
- Aleksandrowicz, O., Vuckovic, M., Kiesel, K., & Mahdavi, A. (2017). Current trends in urban heat island mitigation research: Observations based on a comprehensive research repository. *Urban Climate*, 21, 1–26. <https://doi.org/10.1016/j.uclim.2017.04.002>
- Bader, S., Burgstall, A., Casanueva, A., Duguay-Tetzlaff, A., Gehrig, R., Guber, S., Kotlarski, S., Scherrer, S., & Spirig, C. (2018). Hitze und Trockenheit im Sommerhalbjahr 2018: eine klimatologische Übersicht [Fachbericht]. *Bundesamt für Meteorologie und Klimatologie, MeteoSchweiz*, 272(38). Retrieved from https://www.meteoschweiz.admin.ch/content/dam/meteoswiss/de/service-und-publicationen/Publicationen/doc/Fachbericht_TrockenheitHitze_2018_final_d.pdf
- Brandsma, T., & Wolters, D. (2012) Measurement and statistical modelling of the urban heat island of the city of Utrecht (the Netherlands). *Journal of Applied Meteorology and Climatology* 51(6), 1046-1060. <https://doi.org/10.1175/JAMC-D-11-0206.1>
- Breslin, S. (2018, April 8). *Los Angeles is painting some streets white to counter urban heat island effect*. The Weather Channel. Retrieved from <https://weather.com/news/news/2018-04-10-los-angeles-painting-streets-white>
- Bulkeley, H. (2013). *Cities and climate change*. Routledge. <https://doi.org/10.4324/9780203077207>
- Bundesamt für Statistik. (2020). *Kantonale Szenarien. Szenarien zur Bevölkerungsentwicklung der Schweiz und der Kantone 2020-2050*. Schweizerische Eidgenossenschaft. Retrieved from <https://www.bfs.admin.ch/bfs/de/home/statistiken/bevoelkerung/zukuenftige-entwicklung/kantonale-szenarien.html>
- Burger, M. A. (2020). *Modelling the spatial pattern of the urban heat island of Bern*

- during heatwaves in 2018 and 2019 using a land use regression approach [unpublished Master's thesis]. University of Bern.
- Cerutti, B., Tereanu, C., Domenighetti, G., Cantoni, E., Gaia, M., Bolgiani, I., Lazzaro, M., & Cassis, I. (2006). Temperature related mortality and ambulance service interventions during the heat waves of 2003 in Ticino (Switzerland). *Sozial- und Präventivmedizin*, 51(4), 185–193. <https://doi.org/10.1007/s00038-006-0026-z>
- Copernicus. (2020). *Urban Atlas 2012 [map]*. Retrieved from <https://land.copernicus.eu/local/urban-atlas/urban-atlas-2012>
- Coutts, A. M., Tapper, N., J., Beringer, J., Loughnan, M. & Demuzere, M. (2012). Watering our cities: The capacity for water sensitive urban design to support urban cooling and improve human thermal comfort in the Australian context. *Progress in Physical Geography: Earth and Environment*, 17(1), 2-28. <https://doi.org/10.1177/0309133312461032>
- Deutscher Wetterdienst. (2020). *Urban Heat Islands*. Retrieved from https://www.dwd.de/EN/research/climateenvironment/climate_impact/urbanism/urban_heat_island/urbanheatisland.html.
- Gehrig, R., König, N., & Scherrer, S. (2018). Städtische Wärmeinseln in der Schweiz: klimatologische Studie mit Messdaten in fünf Städten [Fachbericht]. *Bundesamt für Meteorologie und Klimatologie, MeteoSchweiz*, 273(61). Retrieved from https://www.meteoschweiz.admin.ch/content/dam/meteoswiss/de/service-und-publicationen/Publicationen/doc/Fachbericht_273_Staedtische_Waermeinsel_Gehrig_et_al.pdf
- Geletič, J., Lehnert, M., Dobrovolný, P., & Žuvela-Aloise, M. (2019). Spatial modelling of summer climate indices based on local climate zones: Expected changes in the future climate of Brno, Czech Republic. *Climatic Change*, 152. <https://doi.org/10.1007/s10584-018-2353-5>
- Grize, L., Huss, A., Thommen, O., Schindler, C., & Braun-Fahrländer, C. (2005). Heat wave 2003 and mortality in Switzerland. *Swiss Medical Weekly*, 135(13–14), 200–205.
- Grimmond, C. S. B., Roth, M., Oke, T. R., Au Y. C., Best, M., Betts, R., Carmichael, G., Cleugh, H., Dabberdt, W., Emmanuel, R., Freitas, E., Fortuniak, K., Hanna, S., Klein, P., Kalkstein, L. S., Liu, C.H., Nickson, A., Pearlmutter, D., Sailor, D., & Voogt, J. (2010). Climate and more sustainable cities: Climate information for improved planning and management of cities (producers/capabilities

- perspective). *Procedia Environmental Sciences*, 1. 247–274.
<https://doi.org/10.1016/j.proenv.2010.09.016>
- Gubler, M. R., & Brönnimann, S. (2020). *Evaluation and application of a low-cost measurement network to study intra-urban temperature differences during record summer 2018*. Bern Open Repository and Information System.
<https://doi.org/10.7892/boris.140420>
- Hidalgo, J., Masson, V., Baklanov, A., Pigeon, G., & Gimeno, L. (2008). Advances in Urban Climate Modelling. *Annals of the New York Academy of Sciences*, 1146(1), 354–374. <https://doi.org/10.1196/annals.1446.015>
- Hu, Y., White, M., & Ding, W. (2016) An Urban Form Experiment on Urban Heat Island Effect in High Density Area, *Procedia Engineering*, 169, 166-174.
<https://doi.org/10.1016/j.proeng.2016.10.020>
- Jiang, S., Lee, X., Wang, J., & Wang, K. (2019). Amplified urban heat islands during heat wave periods. *Journal of Geophysical Research: Atmospheres*, 124(14), 7797–7812. doi:10.1029/2018jd030230
- Konopacki, S. J., & Akbari, H. (2002). *Energy savings for heat-island reduction strategies in Chicago and Houston*. Lawrence Berkeley National Laboratory.
- Kubota, T., Lee, H. S., Trihamdani, A. R., Phuong, T. T. T., Tanaka, T., & Matsuo, K. (2017). Impacts of land use changes from the Hanoi Master Plan 2030 on urban heat islands: Part 1. Cooling effects of proposed green strategies. *Sustainable cities and society*, 32, 295-317, doi:10.1016/j.scs.2017.04.001
- Li, Y., Schubert, S., Kropp, J. P., & Rybski, D. (2020). On the influence of density and morphology on the Urban Heat Island intensity. *Nature Communications*, 11(2647). <https://doi.org/10.1038/s41467-020-16461-9>
- Mahdavi, A., Kiesel, K., & Vuckovic, M. (2016). Methodologies for UHI Analysis. In F. Musco (Ed.), *Counteracting Urban Heat Island Effects in a Global Climate Change Scenario* (pp. 71-91). Springer, Cham. https://doi.org/10.1007/978-3-319-10425-6_3
- Mathys, H., Maurer, R., Messerli, B., Wanner, H., & Winiger, M. (1980). Klima und Lufthygiene im Raum Bern – Resultate des Forschungsprogramms KLIMUS und ihre Anwendung in der Raumplanung. *Geographisches Institut der Universität Bern, Beiträe zum Klima Der Region Bern*, 10.
<https://doi.org/10.4480/GB2019.G12>

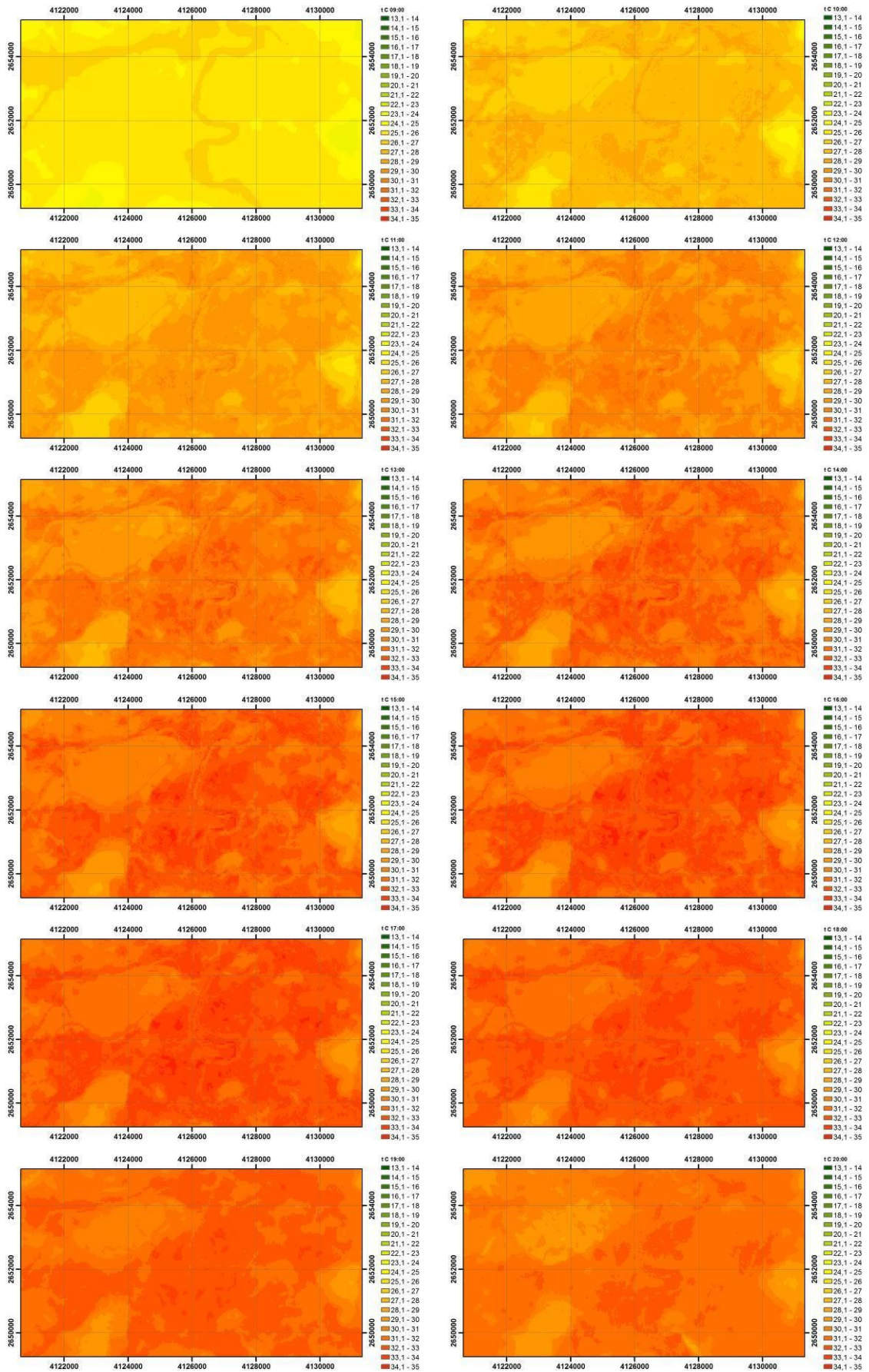
- Musco, F. (Ed.). (2016). *Counteracting Urban Heat Island Effects in a Global Climate Change Scenario*. Springer International.
- National Centre for Climate Services. (2018). *CH2018 – Climate scenarios for Switzerland: Technical report*. Schweizerische Eidgenossenschaft. Retrieved from <https://www.nccs.admin.ch/nccs/en/home/climate-change-and-impacts/swiss-climate-change-scenarios.html>
- Niachou, A., Papakonstantinou, K., Santamouris, M., Tsangrassoulis, A., & Mihalakakou, G. (2001). Analysis of the green roof thermal properties and investigation of its energy performance. *Energy and Buildings*, 33(7), 719–729. [https://doi.org/10.1016/S0378-7788\(01\)00062-7](https://doi.org/10.1016/S0378-7788(01)00062-7)
- Nemec, J., & Žuvela-Aloise, M. (n.d.). *Temperaturunterschiede in der Stadt: Stadtklima der Zukunft in Wien*. Zentralanstalt für Meteorologie und Geodynamik http://www.zamg.ac.at/docs/forschung/klimatologie/temperaturunterschiede_stadtklima_zukunft.pdf
- Oke, T. R. (1973). City size and the urban heat island. *Atmospheric Environment* (1967), 7(8), 769–779. [https://doi.org/10.1016/0004-6981\(73\)90140-6](https://doi.org/10.1016/0004-6981(73)90140-6)
- Oke, T.R. (1980): Climatic impacts of urbanization. In: Bach, W., Pankrath, J., & Williams, J. (Eds.) *Interactions of Energy and Climate*, 339-356. Springer, Dordrecht. https://doi.org/10.1007/978-94-009-9111-8_19
- Oke, T. R. (1982): The energetic basis of the urban heat island. *Quarterly Journal of the Royal Meteorological Society*, 108(455), pp. 1–24.
- Oke, T. R. (1987). *Boundary layer climates* (2nd ed.). Routledge.
- Oke, T. R. (1991). Climate of Cities. In: F. Baer, N. L. Canfield, & J. M. Mitchell (Eds.), *Climate in human perspective* (61-75). Springer, Dordrecht. https://doi.org/10.1007/978-94-011-3320-3_6
- Oke, T. R., Mills, G., Christen, A., & Voogt, J. A. (2017). *Urban climates*. Cambridge University Press. <https://doi.org/10.1017/9781139016476>
- O'Malley, C., Piroozfar, P., Farr, E. R. P., & Pomponi, F. (2015). Urban Heat Island (UHI) mitigating strategies: A case-based comparative analysis. *Sustainable Cities and Society*, 19. 222-235, <https://doi.org/10.1016/j.scs.2015.05.009>.
- Pérez, G., & Perini, K. (Eds.). (2018). *Nature based strategies for urban and building sustainability*. Butterworth-Heinemann, Elsevier. <https://doi.org/10.1016/C2016-0-03181-9>

- Arabi, R., Shahidan, M., Kamal, M., Ja'afar, M.F., & Rakhshandehroo, M. (2015). Mitigating Urban Heat Island Through Green Roofs. *Current World Environment*, 10 (special issue May 2015). <https://doi.org/10.12944/cwe.10.special-issue1.111>
- Ramamurthy, P., & Bou-Zeid, E. (2016). Heatwaves and urban heat islands: A comparative analysis of multiple cities. *Journal of Geophysical Research: Atmospheres*. 122(1), 168–178. <https://doi.org/10.1002/2016JD025357>
- Ren, G., & Zhou, Y. (2014). Urbanization effect on trends of extreme temperature indices of national stations over mainland China, 1961–2008. *Journal of Climate*, 27(6), 2340-2360, <https://doi.org/10.1175/jcli-d-13-00393.1>
- Robitu, M., Musy, M., Inard, C., & Groleau, D. (2006). Modelling the influence of vegetation and water pond on urban microclimate. *Solar Energy*, 80(4), 435–447. <https://doi.org/10.1016/j.solener.2005.06.015>
- Rodatz, M. (2012). Produktive „Parallelgesellschaften“. Migration und Ordnung in der (neoliberalen) „Stadt der Vielfalt“. Productive „Parallel Societies“. Migration and Order in the (neoliberal) „City of Diversity“. *Behemoth*, 5, 70–103. <https://doi.org/10.1515/behemoth.2012.006>
- Rosenfeld, A. H., Akbari, H., Bretz, S., Fishman, B. L., Kurn, D. M., Sailor, D., & Taha, H. (1995). Mitigation of urban heat islands: Materials, utility programs, updates. *Energy and Buildings*, 22(3), 255–265. [https://doi.org/10.1016/0378-7788\(95\)00927-P](https://doi.org/10.1016/0378-7788(95)00927-P)
- Sailor, D. J. (1995). Simulated urban climate response to modifications in surface albedo and vegetative cover. *Journal of Applied Meteorology*, 34(7), 1694–1704. <https://doi.org/10.1175/1520-0450-34.7.1694>
- Santamouris, M. (2014). Cooling the cities: A review of reflective and green roof mitigation technologies to fight heat island and improve comfort in urban environments. *Solar Energy*, 103, 682–703. <https://doi.org/10.1016/j.solener.2012.07.003>
- Shashua-Bar, L., & Hoffman, M. E. (2000). Vegetation as a climatic component in the design of an urban street: An empirical model for predicting the cooling effect of urban green areas with trees. *Energy and Buildings*, 31(3), 221–235. [https://doi.org/10.1016/S0378-7788\(99\)00018-3](https://doi.org/10.1016/S0378-7788(99)00018-3)

- Sievers, U. (1995). Verallgemeinerung der Stromfunktionsmethode auf drei Dimensionen. *Meteorologische Zeitschrift*, 4(1), 3–15. <https://doi.org/10.1127/metz/4/1995/3>
- Sievers, U. (2017). Das kleinskalige Strömungsmodell MUKLIMO_3: Teil 2: Thermodynamische Erweiterungen [user guide]. Deutscher Wetterdienst. Retrieved from https://www.dwd.de/DE/leistungen/pbfb_verlag_berichte/pdf_einzelbaende/248_pdf.pdf?__blob=publicationFile&v=2
- Sievers, U., & Zdankowski, W. G. (1986). A microscale urban climate model. *Contributions to Atmospheric Physics*, 59, 13–40.
- Stadt Bern. (2015). Energie- und Klimastrategie 2025, Stadt Bern: Energie- und klimapolitische Leitlinien 2015-2025. Retrieved from <https://www.bern.ch/politik-und-verwaltung/stadtverwaltung/fpi/immobilien-stadt-bern/nachhaltiges-immobilienmanagement/grundsaeetze/ftw-simplelayout-filelistingblock/energie-und-klimastrategie-2025>
- Stadt Bern. (2017). *STEK 2016: Stadtentwicklungs konzept Bern: Gesamtbericht*. Stadt Bern. Retrieved from <https://www.bern.ch/themen/planen-und-bauen/stadtentwicklung/stadtentwicklungsprojekte/stek-2016/unterlagen/downloads/stek2016-berngesamt-161207-grb-web.pdf>
- Stadt Bern. (2020). *Produktegruppen-Budget 2021: Beschluss des Stadtrats: 17. September 2020*. Retrieved from <https://www.bern.ch/themen/stadt-recht-und-politik/finanzen/budget/downloads/budget-2021-beschluss-sr-web-03.pdf/view>
- Stadt Bern. (n.d.). *Chantier Planungen*. Retrieved from <https://www.bern.ch/themen/planen-und-bauen/stadtentwicklung/stadtentwicklungsprojekte/chantier-planungen>
- Stewart, I. D. (2011). A systematic review and scientific critique of methodology in modern urban heat island literature. *International Journal of Climatology*, 31(2), 200–217. <https://doi.org/10.1002/joc.2141>
- Straka, M., & Sodoudi, S. (2019). Evaluating climate change adaptation strategies and scenarios of enhanced vertical and horizontal compactness at urban scale (a case study for Berlin). *Landscape and Urban Planning*, 183, 68–78. Retrieved from <https://doi.org/10.1016/j.landurbplan.2018.11.006>
- Taha, H. (1997). Urban climates and heat islands: Albedo, evapotranspiration, and anthropogenic heat. *Energy and Buildings*, 25(2), 99–103. [https://doi.org/10.1016/S0378-7788\(96\)00999-1](https://doi.org/10.1016/S0378-7788(96)00999-1)

- Theeuwes, N. E., Solcerová, A., Steeneveld, G. J. (2013). Modelling the influence of open water surfaces on the summertime temperature and thermal comfort in the city. *Journal of Geophysical Research: Atmospheres*, 118(16), 8881–8896. <https://doi.org/10.1002/jgrd.50704>
- UN Department of Economic and Social Affairs. (2018). *World urbanization prospects: The 2018 revision*. United Nations. Retrieved from <https://population.un.org/wup/Publications/Files/WUP2018-Report.pdf>
- University of Wyoming. (n.d.). Observations for Station 06610 starting 1100Z 03 Aug 2018. Retrieved from <http://weather.uwyo.edu/cgi-bin/bufr/aob.py?datetime=2018-08-03%2012:00:00&id=06610&type=TEXT:LIST>
- US Environmental Protection Agency. (2008). *Reducing urban heat islands: Compendium of strategies [draft]*. Retrieved from <https://www.epa.gov/heat-islands/heat-island-compendium>.
- Verein Deutscher Ingenieure. (1994). *Umweltmeteorologie: Wechselwirkung zwischen Atmosphäre und Oberflächen: Berechnung der kurz- und langwelligen Strahlung*. Beuth-Verlag.
- Volker, S. Baumeister, H. Classen, T. Hornberg, C., & Kistemann, T. (2013). Evidence for the temperature-mitigating capacity of urban blue space: A health geographic perspective. *Erdkunde*, 67(4), 355-371.
- Wong, N. H., Jusuf, S. K., Syafii, N. I., Chen, Y., Hajadi, N., Sathyanarayanan, H., & Manickavasagam, Y. V. (2011). Evaluation of the impact of the surrounding urban morphology on building energy consumption. *Solar Energy*, 85(1), 57–71. <https://doi.org/10.1016/j.solener.2010.11.002>
- World Health Organization. (2009). Improving public health responses to extreme weather/heat-waves – EuroHEAT [technical summary]. Retrieved from <https://apps.who.int/iris/bitstream/handle/10665/107935/E92474.pdf?sequence=1&isAllowed=y>
- Žuvela-Aloise, M., Koch, R., Buchholz, S. et al. (2016). Modelling the potential of green and blue infrastructure to reduce urban heat load in the city of Vienna. *Climatic Change* 135, 425–438, <https://doi.org/10.1007/s10584-016-1596-2>
- Žuvela-Aloise, M., Andre, K., Schwaiger, H., Bird, D. N., & Gallaun, H. (2018). Modelling reduction of urban heat load in Vienna by modifying surface properties of roofs. *Theoretical and Applied Climatology*, 131, 1005–1018, <https://doi.org/10.1007/s00704-016-2024-2>

Appendix A



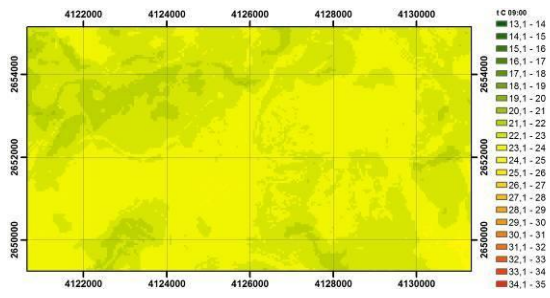


Figure A.1: The model was built for the period from 09:00 on August 3rd, 2018 to 09:00 on August 4th, 2018 with intervals of 1 hour

Appendix B

FID	NORD_CHT	OST_CHT	ELEV_CH	0308201 12	t C 12 0	diff12	0308201 1	t C 16	diff16	04082018 3	t C 03 0	diff03	04082018	t C 07	diff07
0	46.94729	7.43849	542.5	29.252	30.24	-0.988	33.639	32.96	0.679001	22.429	24.66	-2.231	21.664	21.29	0.373999
1	46.95289	7.48707	551.5	30.154	30.85	-0.696	33.848	33.36	0.487999	21.569	24.32	-2.751	20.234	21.06	-0.825999
2	46.93888	7.4503	526.9	29.752	30.81	-1.058	32.807	33.5	-0.693	21.378	24.13	-2.752	19.472	20.66	-1.188
3	46.94065	7.45822	551.6	29.953	29.97	-0.016999	34.691	32.67	2.021	21.378	24.64	-3.262	20.043	20.9	-0.857
4	46.93798	7.45656	535.2	27.173	28.61	-1.437	31.676	31.17	0.506	20.615	24.26	-3.645	18.711	20.51	-1.799
5	46.94318	7.47318	557	29.853	29.76	0.093	32.807	32.42	0.387002	22.333	24.31	-1.977	20.043	20.52	-0.477
6	46.94658	7.43786	540.3	29.552	30.25	-0.698	33.43	32.96	0.470001	22.812	24.75	-1.938	20.805	21.31	-0.504999
7	46.94813	7.45351	532	28.06	30.8	-2.74	31.88	33.45	-1.57	23.388	25.08	-1.692	21.664	21.15	0.514
8	46.94763	7.44028	542.4	28.953	30.18	-1.227	33.639	32.95	0.688999	23.484	24.66	-1.176	21.664	21.33	0.334
9	46.94832	7.43365	540.1	29.352	30.14	-0.787999	34.374	32.83	1.544	22.429	24.2	-1.771	20.805	20.99	-0.185
10	46.94471	7.46442	549.2	29.652	29.27	0.382	32.497	31.91	0.587	21.187	24.25	-3.063	19.377	20.91	-1.533
11	46.94692	7.44354	542.6	29.352	30.07	-0.718	32.911	32.67	0.241002	23.196	25.01	-1.814	21.569	21.41	0.159
12	46.94706	7.45233	534	31.064	30.11	0.953999	33.014	32.74	0.273998	22.333	24.99	-2.657	20.519	20.92	-0.401
13	46.95189	7.46019	568.4	27.961	29.63	-1.669	32.497	32.52	-0.023001	21.473	25.49	-4.017	19.377	21.14	-1.763
14	46.95065	7.46992	579.1	29.652	29.73	-0.077999	33.222	32.29	0.931999	22.717	24.96	-2.243	20.424	20.91	-0.486
15	46.94719	7.42567	543.7	29.053	30.22	-1.167	32.291	32.81	-0.519001	22.525	24.65	-2.125	21.282	21.17	0.112
16	46.9395	7.44213	503.1	30.255	31.12	-0.865001	34.479	33.58	0.898998	21.378	24.08	-2.702	19.282	20.33	-1.048
17	46.94687	7.4562	499.6	29.053	30.95	-1.897	33.848	33.56	0.287999	22.333	24.11	-1.777	20.519	21.42	-0.901
18	46.95791	7.4354	558.6	29.552	30.96	-1.408	32.086	33.89	-1.804	22.908	24.5	-1.592	21.091	21.5	-0.409
19	46.93919	7.48007	553.1	27.37	30.38	-3.01	32.188	32.87	-0.681999	21.473	24.27	-2.797	19.472	20.26	-0.788
20	46.96717	7.46968	547.6	29.152	29.83	-0.678	32.807	32.54	0.266999	22.717	24.37	-1.653	20.996	21.38	-0.383999
21	46.9612	7.45877	555.4	29.352	30.95	-1.598	33.535	33.71	-0.174999	22.812	25.06	-2.248	21.091	21.93	-0.839
22	46.94828	7.40475	544.6	29.352	29.75	-0.398	33.118	32.4	0.717998	21.855	21.98	-0.125	19.758	20.14	-0.381999
23	46.95292	7.42253	553.8	29.352	30.37	-1.018	33.118	33.08	0.037998	22.812	24.22	-1.408	21.187	20.93	0.257
24	46.9356	7.46954	544.6	29.953	30.76	-0.807	34.903	33.45	1.453	20.996	24.65	-3.654	19.092	20.42	-1.328
25	46.94211	7.41689	548.4	29.252	29.38	-0.127999	33.118	31.92	1.198	20.71	23.24	-2.53	19.282	20.77	-1.488
26	46.94333	7.40633	555.5	28.655	29.79	-1.135	32.911	32.43	0.481	22.238	23.21	-0.971999	20.519	21.03	-0.511001
27	46.9402	7.38371	561.9	29.152	30.46	-1.308	33.43	33.05	0.380001	20.615	24.69	-4.075	19.092	21.1	-2.008
28	46.92607	7.43739	619.8	28.853	29.25	-0.397	33.326	31.96	1.366	20.996	24.95	-3.954	19.472	21.15	-1.678
29	46.95896	7.44514	538.1	28.953	30.41	-1.457	33.118	33.26	-0.141998	22.525	24.28	-1.755	21.187	21.44	-0.253001
30	46.95739	7.42128	552.3	27.567	28.56	-0.992999	31.268	31.14	0.128001	19.662	21.95	-2.288	18.045	19.59	-1.545
31	46.96174	7.45191	554.9	28.357	31.24	-2.883	33.326	34.17	-0.843998	23.966	25.19	-1.224	21.473	21.92	-0.447
32	46.95696	7.45802	559.3	27.764	30.58	-2.816	33.743	33.29	0.452999	22.812	24.73	-1.918	20.996	21.64	-0.643999
33	46.94187	7.43462	521.4	28.06	31.01	-2.95	31.983	33.67	-1.687	21.664	24.88	-3.216	19.758	21.48	-1.722
34	46.95519	7.44772	542.8	28.258	30.34	-2.082	33.639	33.22	0.418999	23.388	25.02	-1.632	20.996	21.55	-0.553999
35	46.92781	7.42031	567.2	29.053	29.89	-0.836999	32.6	32.47	0.129999	20.901	24.74	-3.839	19.377	20.38	-1.003
36	46.94828	7.44741	539.5	28.456	30.16	-1.704	32.188	32.8	-0.611999	22.717	25.01	-2.293	20.901	21.57	-0.669
37	46.96156	7.45566	555	29.053	31.04	-1.987	33.222	33.84	-0.618	24.255	25.41	-1.155	22.142	21.95	0.191999
38	46.968	7.46248	550.5	28.953	30.4	-1.447	32.807	33.1	-0.292998	23.388	24.6	-1.212	20.901	21.23	-0.329
39	46.9651	7.43821	573.1	29.053	29.14	-0.086999	32.6	31.69	0.909999	21.473	25	-3.527	19.853	21.34	-1.487
40	46.93861	7.44738	519.7	30.255	31.37	-1.115	33.222	34.12	-0.897999	21.951	24.18	-2.229	20.424	21.45	-1.026
41	46.9448	7.42713	528.6	30.154	30.72	-0.565999	34.903	33.36	1.543	23.004	24.59	-1.586	21.378	21.27	0.108
42	46.94714	7.46407	561.6	30.255	30.86	-0.605001	33.326	33.64	-0.313999	22.046	24.91	-2.864	20.043	21.07	-1.027
43	46.96766	7.44922	526.8	29.452	30.5	-1.048	33.953	33.29	0.662999	20.615	23.02	-2.405	19.187	20.19	-1.003
44	46.93719	7.42312	560.6	29.652	30.52	-0.868	34.268	33.16	1.108	21.473	24.08	-2.607	19.853	20.78	-0.927001
45	46.95765	7.46791	559.7	28.754	30.27	-1.516	33.639	32.97	0.668999	23.581	25.15	-1.569	20.329	21.35	-1.021
46	46.95152	7.44077	534.6	29.752	30.07	-0.318	33.848	32.7	1.148	23.292	24.44	-1.148	21.716	21.39	0.370001
47	46.94896	7.45103	527.6	30.054	30.52	-0.466	33.014	33.24	-0.226002	22.333	24.65	-2.317	20.519	21.27	-0.751
48	46.94861	7.38906	557.8	28.754	30.44	-1.686	31.472	33.05	-1.578	22.525	23.35	-0.825	19.853	20.98	-1.127
49	46.92714	7.45173	556.4	30.054	30.79	-0.736001	34.374	33.28	1.094	21.951	25.02	-3.069	20.996	21.32	-0.324
50	46.94495	7.43455	529.3	29.053	30.79	-1.737	34.058	33.61	0.447999	22.717	24.73	-2.013	20.996	21.42	-0.424
51	46.94302	7.39587	556.7	27.665	30.57	-2.905	32.497	33.17	-0.672998	22.429	23.64	-1.211	20.424	21.35	-0.926
52	46.9371	7.44306	503.8	27.862	29.96	-2.098	33.535	32.47	1.065	19.948	23.26	-3.312	18.426	20.08	-1.654
53	46.974	7.44116	492.4	29.953	30.35	-0.397	34.268	33.27	0.998	20.805	22.99	-2.185	19.187	20.23	-1.043
54	46.94077	7.43133	525.7	29.252	31.22	-1.968	34.163	33.73	0.433	22.525	24.86	-2.335	20.805	21.62	-0.815001
55	46.9489	7.40134	545.9	29.752	30.58	-0.828	33.953	33.21	0.743001	21.187	22.45	-1.263	19.567	21.04	-1.473
56	46.94555	7.37478	554.2	29.352	30.21	-0.857999	33.848	32.94	0.908001	21.091	22.73	-1.639	18.711	20.18	-1.469
57	46.95575	7.49872	574.3	29.552	29.85	-0.296	33.326	32.53	0.796001	22.621	24.78	-2.159	20.996	20.89	0.106001
58	46.96882	7.50376	557.6	28.853	29.48	-0.627	33.014	32.15	0.863998	20.329	23.2	-2.871	18.616	19.5	-0.884
59	46.95029	7.42015	552.4	29.152	29.04	0.111999	32.807	31.64	1.167	21.378	22.6	-1.222	19.472	20.67	-1.198
60	46.9478	7.43686	540.1	30.659	30.03	0.628999	35.222	32.82	2.402	22.908	24.8	-1.892	21.187	21.22	-0.032999
61	46.93122	7.45326	533.5	30.659	30.58	0.079	33.953	33.12	0.833001	21.187	24.07	-2.883	19.092	19.35	-0.258
62	46.94994	7.41532	550.5	28.853	30.01	-1.157	32.6	32.71	-0.109999	23.1	23.17	-0.07	20.329	20.75	-0.421
63	46.94446	7.44571	500.8	28.655	30.21	-1.555	33.118	32.85	0.268002	21.473	24.2	-2.727	19.758	21.23	-1.472
64	46.93508	7.43887	532.6	29.552	30.1	-0.548	34.163	32.67	1.493	21.569	23.7	-2.131	19.853	21.16	-1.307
65	46.95292	7.44847	549.9	30.457	30.74	-0.283	33.118	33.36	-0.242001	23.196	24.65	-1.454	20.996	21.1	-0.104
66	46.96312	7.46255	554.5	30.154	30.58	-0.426	33.43	33.29	0.139999	22.717	24.13	-1.413	20.996	21.52	-0.524

Figure B.1: Simulated temperature, measured temperature, difference between them on 12:00, 16:00, 03:00, 07:00

Appendix C

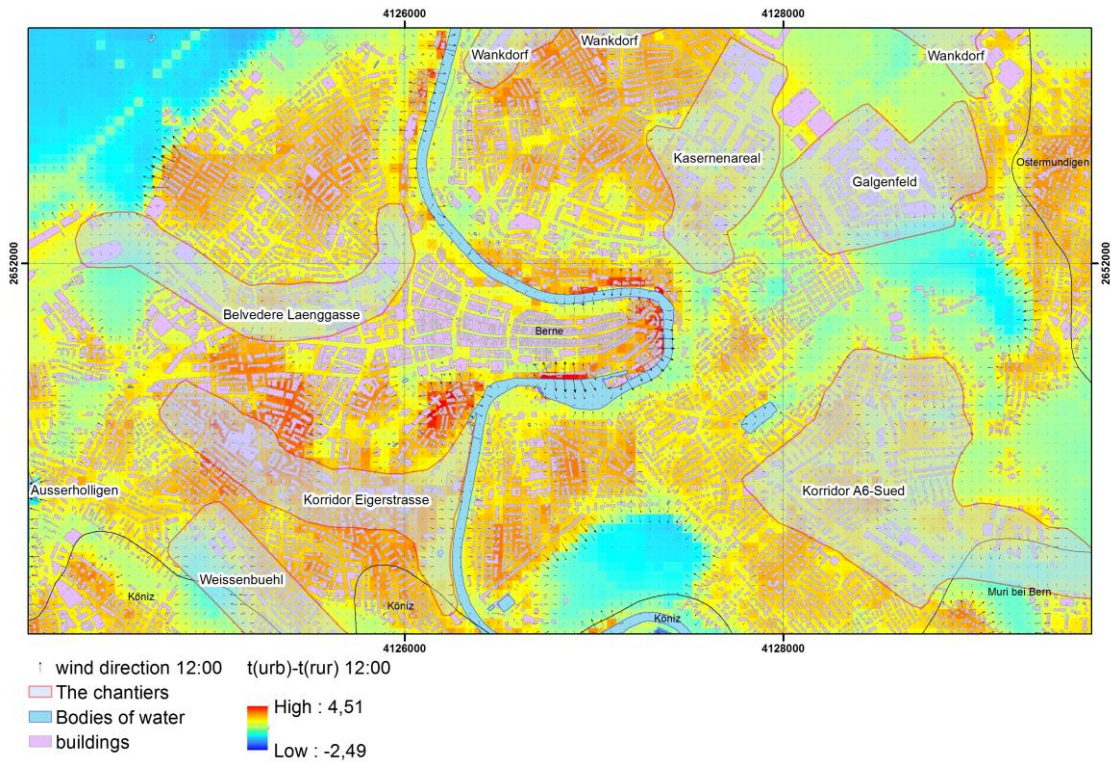


Figure C.1: Chantier map: chantire contours superimposed on grid UHI at 12:00

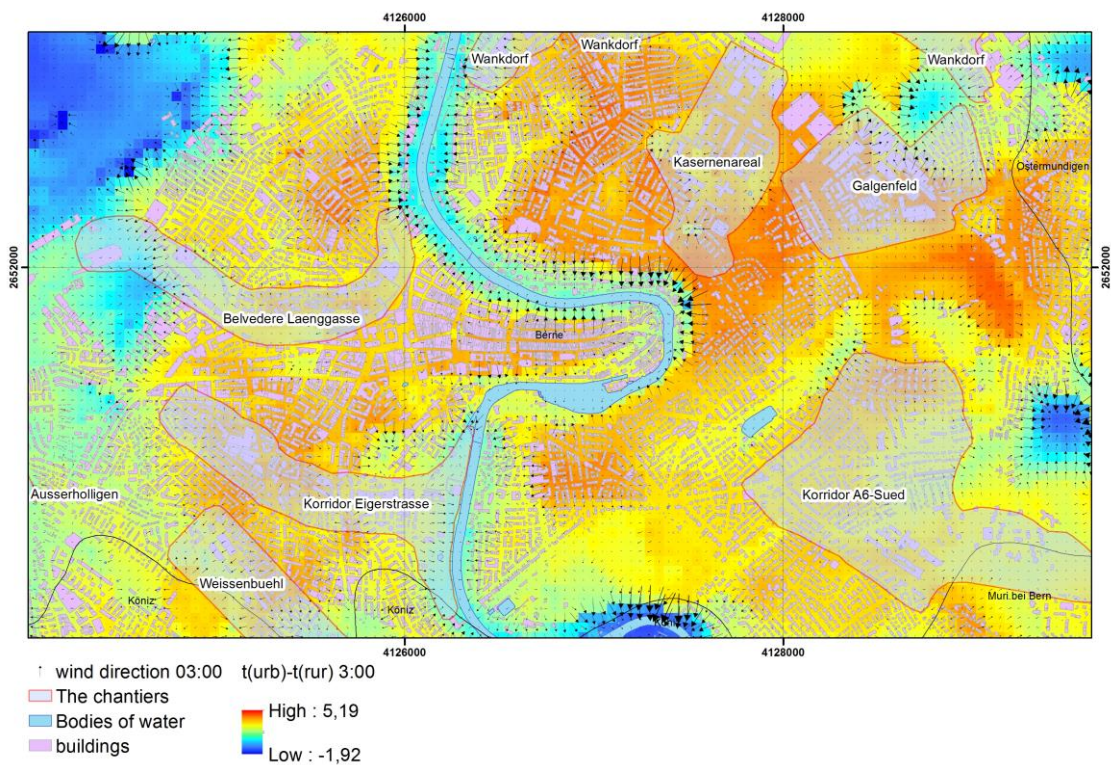


Figure C.2: Chantier map: chantier contours superimposed on grid UHI at 03:00

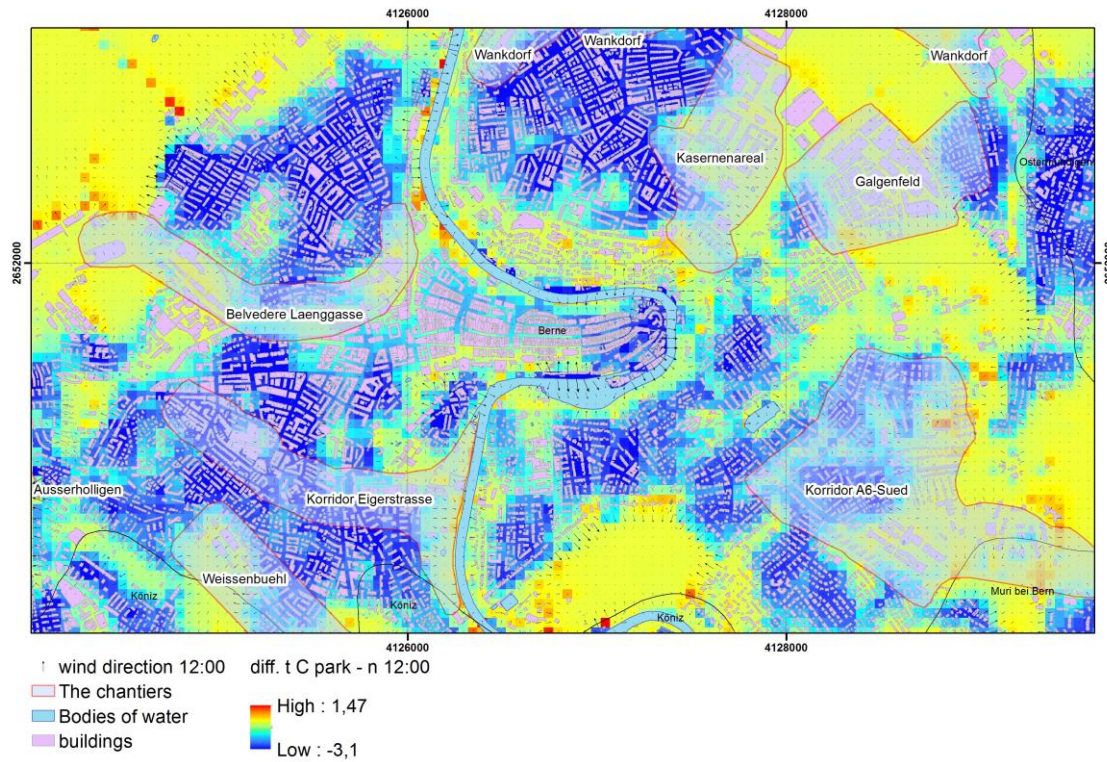


Figure C.3: Chantier map: temperature difference (in °C) between GR and REF at 12:00

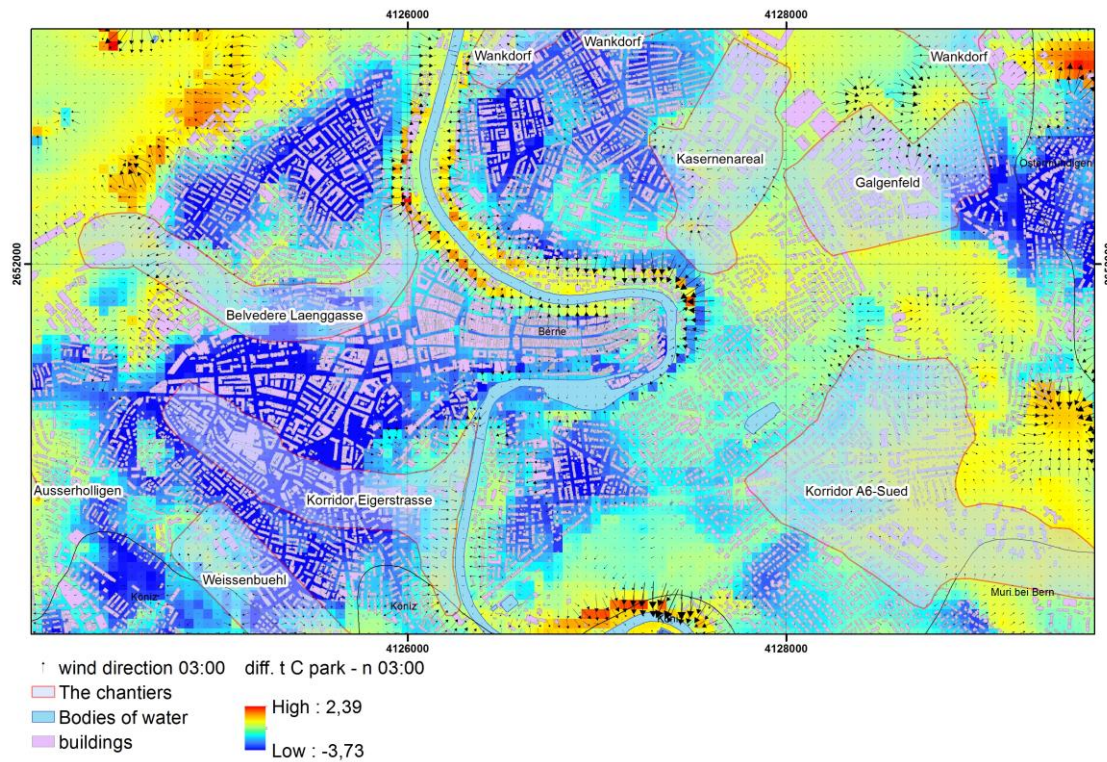


Figure C.4: Chantier map: temperature difference (in °C) between GR and REF at 03:00

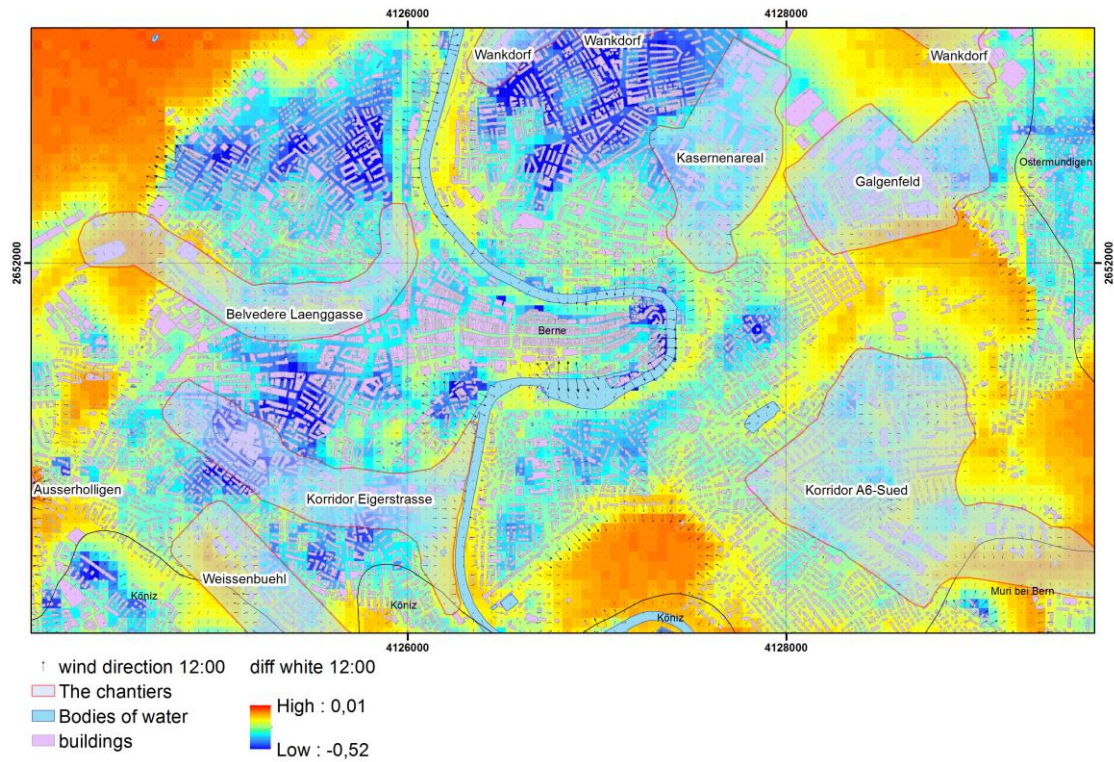


Figure C.5: Chantier map: temperature difference (in °C) between ALB and REF at 12:00

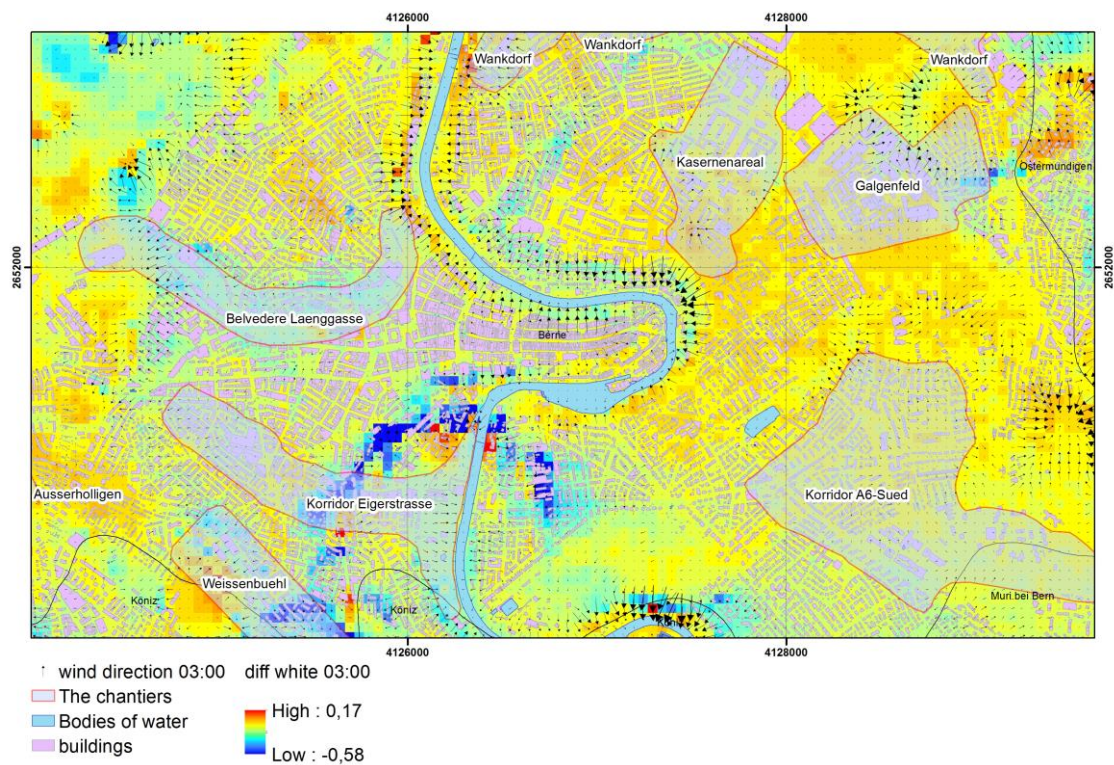


Figure C.6: Chantier map: temperature difference (in °C) between ALB and REF at 03:00

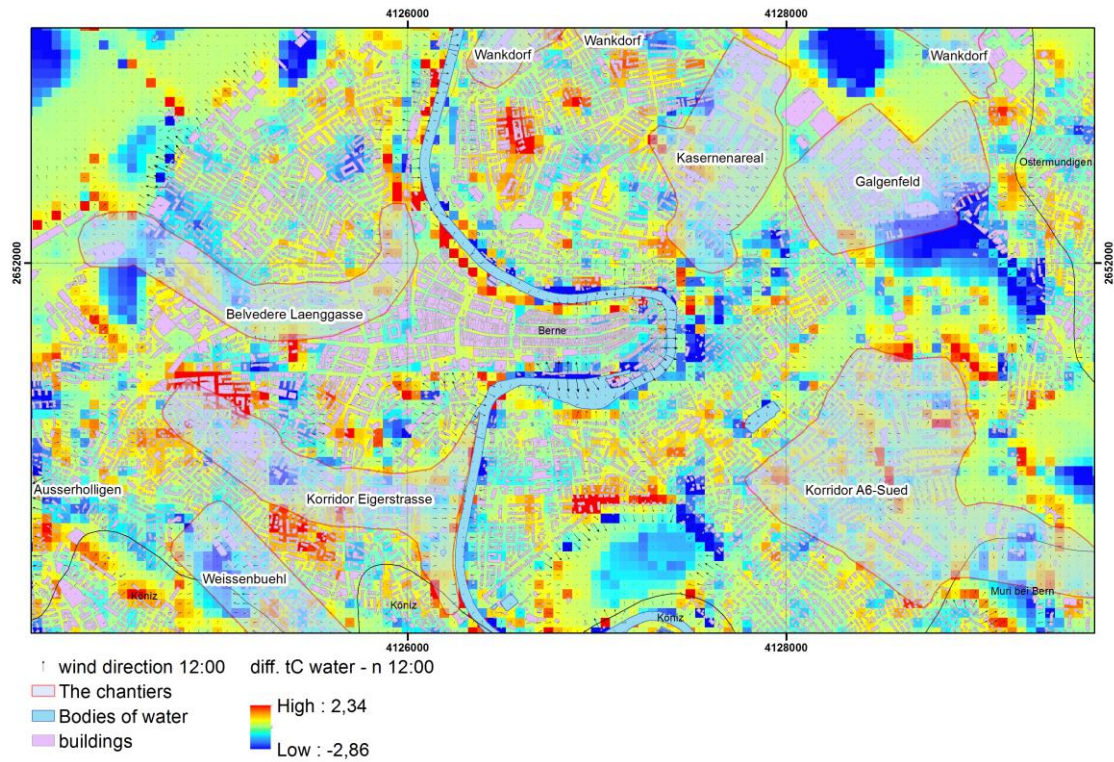


Figure C.7: Chantier map: temperature difference (in °C) between BL and REF at 12:00

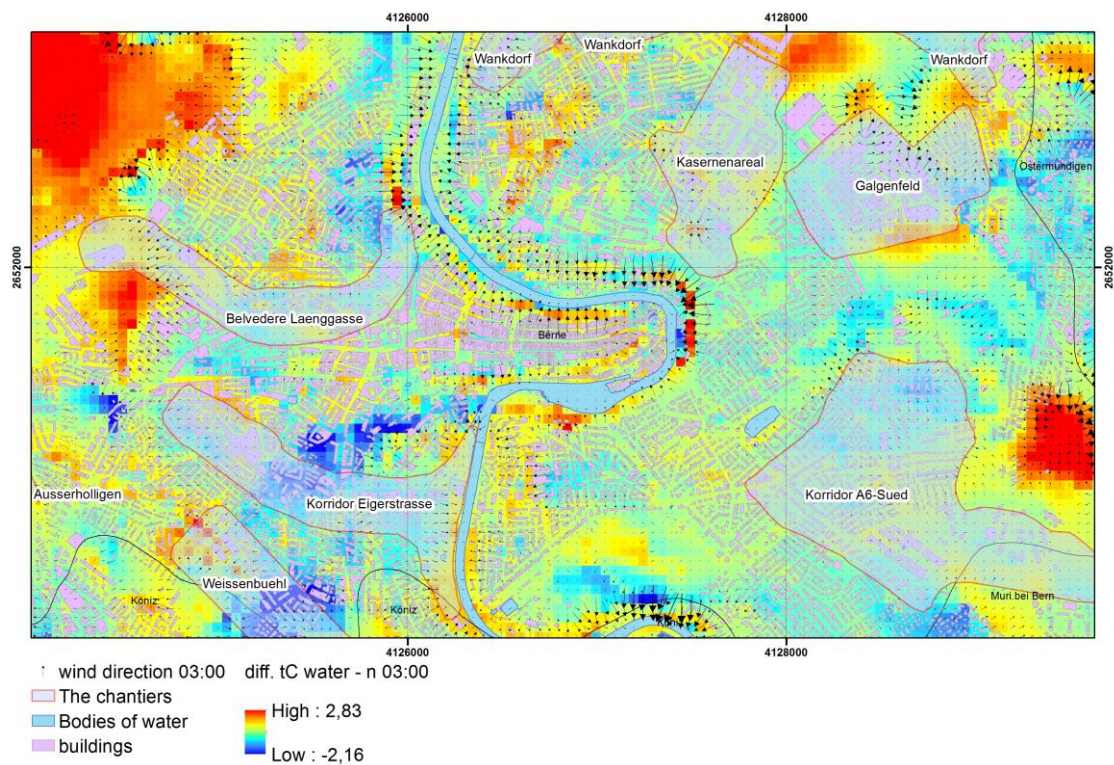


Figure C.8: Chantier map: temperature difference (in °C) between BL and REF at 03:00

Declaration of consent

on the basis of Article 30 of the RSL Phil.-nat. 18

Name/First Name: Antonowa Sofya

Registration Number: 16-129-959

Study program: MSc in Geography

Bachelor Master Dissertation

Title of the thesis: IMPLEMENTATION OF THE URBAN CLIMATE MODEL MUKLIMO_3 FOR BERN AND EVALUATION OF MITIGATION STRATEGIES FOR THE URBAN HEAT ISLAND

Supervisor: Prof. Dr. Stefan Brönnimann

I declare herewith that this thesis is my own work and that I have not used any sources other than those stated. I have indicated the adoption of quotations as well as thoughts taken from other authors as such in the thesis. I am aware that the Senate pursuant to Article 36 paragraph 1 litera r of the University Act of 5 September, 1996 is authorized to revoke the title awarded on the basis of this thesis.

For the purposes of evaluation and verification of compliance with the declaration of originality and the regulations governing plagiarism, I hereby grant the University of Bern the right to process my personal data and to perform the acts of use this requires, in particular, to reproduce the written thesis and to store it permanently in a database, and to use said database, or to make said database available, to enable comparison with future theses submitted by others.

Baden, 29.11.2020

Place/Date

Signature

